Explicit formulas for the asymptotic variance of a linearized model of a Gaussian disturbance driven power system with a uniform damping-inertia ratio

Wu, Xian; Xi, Kaihua; Cheng, Aijie; Lin, Hai Xiang; van Schuppen, Jan H.; Zhang, Chenghui

DOI
10.1016/j.chaos.2024.115511

Publication date
2024

Document Version
Final published version

Published in
Chaos, Solitons and Fractals

Chaos, Solitons and Fractals 188 (2024) 115511

Contents lists available at ScienceDirect

Chaos, Solitons and Fractals

journal homepage: www.elsevier.com/locate/chaos

Explicit formulas for the asymptotic variance of a linearized model of a Gaussian disturbance driven power system with a uniform damping-inertia ratio☆

Xian Wu [a], Kaihua Xi [a,*], Aijie Cheng [a], Hai Xiang Lin [b,c], Jan H. van Schuppen [b], Chenghui Zhang [d]

[a] School of Mathematics, Shandong University, 250100, Jinan, Shandong, China
[b] Delft Institute of Applied Mathematics, Delft University of Technology, 2628 CD, Delft, The Netherlands
[c] Institute of Environmental Sciences (CML), Leiden University, 2333 CC, Leiden, The Netherlands
[d] School of Control Science and Engineering, Shandong University, 250061, Jinan, Shandong, China

ARTICLE INFO

Keywords:
Power systems
Synchronization stability
Invariant probability distribution
Fluctuation propagation
Stochastic Gaussian system
Lyapunov equation

ABSTRACT

Serious fluctuations caused by disturbances may lead to instability of power systems. With the disturbance modeled by a Brownian motion process, the fluctuations are often described by the asymptotic variance at the invariant probability distribution of an associated Gaussian stochastic process. Here, we derive the explicit formula of the variance matrix for the system with a uniform damping-inertia ratio at all the nodes, which enables us to analyze the influences of the system parameters on the fluctuations and investigate the fluctuation propagation in the network. With application to systems with complete graphs and star graphs, it is found that the variance of the frequency at the disturbed node is significantly bigger than those at all the other nodes. It is also shown that adding new nodes may prevent the propagation of fluctuations from the disturbed node to all the others. Finally, it is proven theoretically that larger line capacities accelerate the propagation of the frequency fluctuation and larger inertia of synchronous machines help suppress the fluctuations of the phase differences, however, these acceleration and suppression are quite limited.

1. Introduction

A power system consists of synchronous machines, transmission lines and power supply and demand. The electricity system needs the frequency to be synchronized in order to operate properly. All synchronous machines, such as steam or gas turbine rotor-generators, need to operate with frequencies equal to or very close to the nominal frequency, typically 50 Hz or 60 Hz [1]. Here, the frequency is the rotating phase's derivative, and it equals the synchronous machine's rotational speed, measured in rad/s. Synchronization stability, also known as transient stability in the field of power systems research, refers to the ability to maintain synchronization subjected to disturbances. The electrical system is experiencing an unprecedented threat of losing synchronization as a result of the expansion of the integration of renewable energy sources, which are inherently more vulnerable to unpredictable disturbances.

Here, we focus on the relation of synchronous stability with the variance of the disturbances. The relation depends on the power system parameters in particular upon: the damping and the inertia coefficients of the synchronous machines, the susceptance in the transmission lines, the power supply and demands and the network topology and so on. Based on the analysis of the existence condition [2–4], the small signal stability [5] and the basin attraction of the synchronous state [6–8], the synchronization stability may be improved by changing these parameters, such as changing the inertia of the synchronous machines [9], controlling the power flows in the network [10], adding or deleting transmission lines [11]. This analysis focuses on the synchronous state, in which the disturbances have not yet been explicitly considered in the mathematical model. However, in practice, due to continuously occurring disturbances, the state always fluctuates around a synchronous state. If the state experiences large variations and cannot recover and return to the basin attraction of the synchronous state, then

☆ This work was funded by the Natural Science Foundation of China with Grant No. 62103235, and the Foundation for Innovative Research Groups of the National Natural Science Foundation of China with Grant No. 61821004, and the Key Program of the National Natural Science Foundation of China with Grant No. 62133008.

* Corresponding author.
E-mail addresses: xianwu@mail.sdu.edu.cn (X. Wu), kxi@sdu.edu.cn (K. Xi), aijie@sdu.edu.cn (A. Cheng), H.X.Lin@tudelft.nl (H.X. Lin), j.h.van.schuppen@tudelft.nl (J.H. van Schuppen), zchui@sdu.edu.cn (C. Zhang).

https://doi.org/10.1016/j.chaos.2024.115511
Received 4 May 2024; Received in revised form 5 September 2024; Accepted 6 September 2024
Available online 12 September 2024

the system will lose the synchronization. Thus, the severity of the state fluctuations caused by disturbances directly determines the ability to maintain synchronization.

To suppress the fluctuations, the key is to define such a metric that can reflect the impacts of the system parameters on the propagation of the fluctuations in the system. The $\mathcal{H}_2$ norm defined for an input–output system, which treats the disturbances as inputs and the phase differences and the frequency deviation as outputs, has been used to measure the severity of the fluctuations [9,12–18]. Although it is hard to derive the analytic formula of the $\mathcal{H}_2$ norm due to the heterogeneity of the system parameters, significant insights on suppressing the fluctuations have been obtained from the formulas of the $\mathcal{H}_2$ norm under homogeneous assumptions on the system parameters, e.g., [14–19]. By minimizing this norm, parts of the system parameters such as the inertia and primary control gain can be assigned to suppress the fluctuations in the frequency and the phase difference [9]. In particular, this norm is also used to study the transient performance of the system with the disturbance modeled by colored noise [19]. To avoid the assumption of the uniform damping-inertia ratio, which allows the deduction of the analytic formula of the $\mathcal{H}_2$ norm, a matrix perturbation approach is proposed for the optimal placement of inertia and primary control [20]. With a more realistic metric of Rate of Change of Frequency (RoCoF), the propagation of the fluctuation in the network and the impact of the placement of the inertia on the propagation are investigated in [21]. In physics, the propagation of the fluctuations is also widely investigated [22–26] with various metrics. For example, the variance of these fluctuations can be calculated statistically via simulations with the disturbances modeled by either Gaussian or non-Gaussian noises [22]. By the perturbation method, the arrival time of a disturbance at a node are estimated in [24] in order to investigate the propagation of the disturbance in the network. A new metric is defined in [27] to find susceptible nodes and lines in the network. With the amplitude of the response at the nodes as a metric, emergent complex response pattens across the network are investigated in [26]. From these studies, important insights on the role of the system parameters, such as the inertia and damping of the synchronous machines, the network topology, on the propagation of the disturbances are obtained, which are helpful on tuning the system parameter for real networks.

With the disturbance modeled by a Brownian motion process in the linearized system of the nonlinear power system, the asymptotic variance matrix in the invariant probability distribution of the corresponding stochastic process is used to characterize the fluctuations in the phase difference in each line and the frequency at each node [28,29]. Its analytic formula clearly reveals the relationship between the system parameters and the fluctuations, and the correlation between the phase differences and the frequencies. It also describes how a disturbance propagates in the network. In contrast, the $\mathcal{H}_2$ norm, which is a scalar and equals to the trace of the variance matrix, cannot provide such detailed information. Based on this variance matrix and the synchronous state, a quantitative optimization framework has been proposed in [30]. This variance matrix can be computed from a Lyapunov equations [28,31], which has a very high computing complexity. With this formula, the fluctuations can be effectively suppressed by optimally configuring the system parameters. Due to the heterogeneity of the system parameters and the non-linearity of the system, this explicit formula still has not been derived, which is also a hard problem.

With the assumption of uniform disturbance-damping ratio among the nodes, in which the ratio of the strength of the disturbances and the damping coefficients are all identical at the nodes, formulas of the variance matrix have been deduced in [28]. The relationship between system parameters and fluctuations are partly explored by these formulas. By means of these formulas, the dependence of the fluctuations on the system parameters are partly explored. However, because of the assumption, how the disturbances supplied to nodes propagate through the power network and hence affect the phase differences and the frequencies of all nodes cannot be revealed. In this paper, we deduce the formula for the variance matrix under an assumption of uniform damping-inertia ratios at the nodes. This formula enables us to explore the propagation of the fluctuations throughout the network.

The contributions of this paper to the stability analysis of power systems include:

(i) under the assumption of the uniform damping-to-inertia ratio at all the nodes, we derive analytic expressions of the variance matrices of the phase differences in lines and the frequency at nodes;
(ii) based on the formulas, we analyze the propagation of the disturbances, and investigate the reliance of the propagation on the various system parameters, including the damping and inertia of the synchronous machines, the capacity of lines and the size of networks in special graphs, i.e., complete graphs and star graphs.

This paper is organized as follows. In Section 2, elementary preliminaries on graph theory and the invariant probability distribution of Gaussian process are provided. The problem formulation and the main results of this paper are presented in Sections 3 and 4 respectively. Section 5 provides proofs of the results and Section 6 concludes with remarks.

2. Preliminaries

The elementary notation, properties of graphs and the concept of the asymptotic variance of a stochastic Gaussian system are introduced in this section.

2.1. Notations

The set of the real numbers and the set of the strictly positive real numbers are denoted by $\mathbb{R}$ and $\mathbb{R}_+$ respectively. The vector space of n-tuples of the real numbers is denoted by $\mathbb{R}^n$ for an integer n. For the integers $n,\ m$ the set of n by m matrices with entries of the real numbers, is denoted by $\mathbb{R}^{n\times m}$. Denote the identity matrix of size n by n by $\mathbf{I}_n \in \mathbb{R}^{n\times n}$, the zero vector by $\mathbf{0}_n$, the vector with all elements equal to one by $\mathbf{1}_n$, which may also be denoted by $\mathbf{I}$, $\mathbf{0}$ and $\mathbf{1}$ respectively if the size is clear from the context.

Denote subsets of matrices according to: for an integer n, $\mathbb{R}^{n\times n}_{spd}$ denotes the subset of symmetric positive semi-definite matrices of which an element is denoted by $0 \preceq \mathbf{Q} = \mathbf{Q}^\top$; $\mathbb{R}^{n\times n}_{ortg}$ the subset of orthogonal matrices which by definition satisfy $\mathbf{U}\,\mathbf{U}^\top = \mathbf{I}_n = \mathbf{U}^\top\,\mathbf{U}$. Call a square matrix $\mathbf{A} \in \mathbb{R}^{n\times n}$ *Hurwitz* if all eigenvalues have a real part which is strictly negative, in terms of notation, for any eigenvalue $\lambda(\mathbf{A})$ of the matrix $\mathbf{A}$, $\mathrm{Re}(\lambda(\mathbf{A})) < 0$. For a matrix $\mathbf{A}$, denote the element at the entry (i,j) by $a_{i,j}$.

2.2. Graphs

Denote an undirected weighted graph by $\mathcal{G} = (\mathcal{V}, \mathcal{E})$ with a set of n nodes denoted by $\mathcal{V}$ and a set of m edges or lines denoted by $\mathcal{E}$ and line weight $w_{i,j} = w_{j,i} \in \mathbb{R}_+$ if the nodes i and j are connected and $w_{i,j} = 0$ otherwise. Denote by $k = (i,\ j) \in \mathcal{E}$ the edge connecting the nodes i and j which edge is also denoted by e_k. The Laplacian matrix of the graph with weight $w_{i,j}$ of line (i,j) is defined as $\mathbf{L} = (l_{i,j}) \in \mathbb{R}^{n\times n}$ with

$$l_{i,j} = \begin{cases} -w_{i,j}, & \text{if } i \neq j, \\ \sum_{k=1,\ k\neq i}^{n} w_{i,k}, & \text{if } i = j. \end{cases}$$

The incidence matrix is defined as $\widetilde{\mathbf{C}} = (c_{i,k}) \in \mathbb{R}^{n\times m}$ with $c_{i,k} \in \mathbb{R}$,

$$c_{i,k} = \begin{cases} 1, & \text{if node } i \text{ is the beginning of line } e_k, \\ -1, & \text{if node } i \text{ is the end of line } e_k, \\ 0, & \text{otherwise.} \end{cases} \tag{1}$$

Here the direction of line e_k is arbitrarily specified in order to define the incidence matrix. For the elementary properties of the Laplacian matrix, we refer to [32].

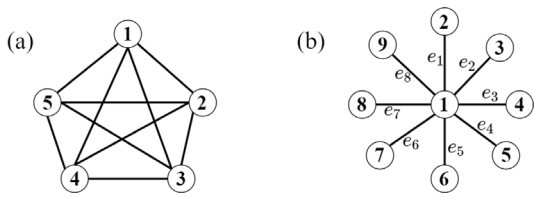

Fig. 1. (a) A complete graph with 5 nodes. (b) A star graph with 9 nodes.

The definitions of complete graphs and star graphs are described below.

Definition 2.1. Consider the graph $\mathcal{G} = (\mathcal{V}, \mathcal{E})$.

(i) If each pair of nodes is connected by a line, then call this graph a complete graph.
(ii) If the graph is a tree and there is a root node which is directly connected to all the other nodes, then call this graph a star graph.

For both a complete graph and a star graph, the form of the incidence matrix depends on the indices of the lines. For convenience of expression, we define the indices for the nodes and lines as below.

Definition 2.2. Consider the graph $\mathcal{G} = (\mathcal{V}, \mathcal{E})$.

(i) If $\mathcal{G}$ is a complete graph, then the indices of the line (i, j) with $i < j$ is defined according to the Lexicographic order.
(ii) If $\mathcal{G}$ is a star graph, the index of the root node is defined as $i = 1$ and the indices of the other nodes are defined as $i = 2, \dots, n$. The indices of the line $(1, k+1)$ are defined as e_k for $k = 2, \dots, n-1$.

An example of a complete graph and an example of a star graph with such indices are shown in Fig. 1.

3. Problem formulation

The power network can be described by a graph $\mathcal{G}(\mathcal{V}, \mathcal{E})$ with node set $\mathcal{V}$ and line set $\mathcal{E} \subset \mathcal{V} \times \mathcal{V}$. A node represents a bus and a line (i, j) represents the transmission line between node i and j. We focus on the transmission network and assume the lines are lossless. The number of nodes in $\mathcal{V}$ and edges in $\mathcal{E}$ are denoted by n and m respectively. The dynamics of the power system are described by the equations [6,33,34],

$$\dot{\delta}_i = \omega_i, \tag{2a}$$

$$m_i\dot{\omega}_i = P_i - d_i\omega_i - \sum_{j=1}^{n} K_{i,j}\sin(\delta_i - \delta_j), \tag{2b}$$

where δ_i and ω_i represent the phase and the frequency deviation of the synchronous generator at node i; $m_i > 0$ and $d_i > 0$ describes the inertia and damping with droop control of the synchronous machine; P_i represents power generation if $P_i > 0$ and denotes power load otherwise; $K_{i,j} = \hat{b}_{ij}V_iV_j$ denotes the effective susceptance with $\hat{b}_{i,j}$ being the susceptance of the line (i, j) and V_i is the voltage at bus i;

In this definition, the voltage dynamics are not considered, which is assumed to be constant. This is practical because the voltage can be controlled in a short time-scale thus can be approximated as constant in the time-scale of the frequency.

When the graph is complete, and $d_i = 1$ for all the nodes and $K_{i,j} = K/n$ for all $(i, j) \in \mathcal{E}$ with $K \in \mathbb{R}_+$, the system becomes *the second-order Kuramoto Model* [35].

Definition 3.1. Define a *synchronous state* of the power system (2) as the vector $\left(\delta^*(t), \omega^*(t)\right)$ with $\boldsymbol{\delta}^*(t) = \widetilde{\boldsymbol{\delta}} + (\widetilde{\omega}t)\mathbf{1}_n \in \mathbb{R}^n$ and $\omega^*(t) = \widetilde{\omega}\mathbf{1}_n \in \mathbb{R}^n$, which is a solution of the equation

$$d_i\widetilde{\omega} = P_i + \sum_{j=1}^{n} K_{i,j}\ \sin(\widetilde{\delta}_j - \widetilde{\delta}_i),\ \text{for } i = 1, \dots, n, \tag{3}$$

and $\widetilde{\delta} = \mathrm{col}(\widetilde{\delta}_i) \in \mathbb{R}^n$ that satisfies $\widetilde{\delta}_i - \widetilde{\delta}_j = (\delta_i^*(t) - \delta_j^*(t))(mod(2\pi))$ for all $(i, j) \in \mathcal{E}$.

By summing all the equations in (3), it yields that at the synchronous state,

$$\widetilde{\omega} = \frac{\sum_i^n P_i}{\sum_i^n d_i} \in \mathbb{R}. \tag{4}$$

The existence of a synchronous state can typically be obtained by increasing the coupling strength $K_{i,j}$ for all the lines to sufficiently high values [2].

The derivation of the linearized system of (2) is briefly summarized below with an assumption for the synchronous state.

Assumption 3.2. Consider the system (2), assume that (1) the graph $\mathcal{G}$ is connected, hence $m \geq n-1$ holds; (2) there exists a synchronous state $\left(\boldsymbol{\delta}^*(t), \mathbf{0}\right)$ such that the phase differences $|\widetilde{\delta}_i - \widetilde{\delta}_j| < \pi/2$ for all $(i, j) \in \mathcal{E}$.

The *linearized system* of (2), linearized around the considered synchronous state, is then derived

$$\begin{pmatrix} \dot{\boldsymbol{\delta}} \\ \dot{\boldsymbol{\omega}} \end{pmatrix} = \begin{pmatrix} 0 & \mathbf{I}_n \\ -\mathbf{M}^{-1}\mathbf{L} & -\mathbf{M}^{-1}\mathbf{D} \end{pmatrix} \begin{pmatrix} \boldsymbol{\delta} \\ \boldsymbol{\omega} \end{pmatrix} = \mathbf{J} \begin{pmatrix} \boldsymbol{\delta} \\ \boldsymbol{\omega} \end{pmatrix}, \tag{5}$$

where $\boldsymbol{\delta} = \mathrm{col}(\delta_i) \in \mathbb{R}^n$, $\boldsymbol{\omega} = \mathrm{col}(\omega_i) \in \mathbb{R}^n$, $\mathbf{D} = \mathrm{diag}(d_i) \in \mathbb{R}^{n\times n}$, $\mathbf{M} = \mathrm{diag}(m_i) \in \mathbb{R}^{n\times n}$, and $\mathbf{L} \in \mathbb{R}^{n\times n}$ is the Laplacian matrix of the graph with the weight $w_{i,j} = K_{i,j}\cos\delta_{ij}^*$ for the line (i, j), generated by $(\boldsymbol{\delta}^*, \mathbf{0})$ with $\delta_{ij}^* = \delta_i^* - \delta_j^*$, $\mathbf{J} \in \mathbb{R}^{2n\times 2n}$ is also called *the Jacobian matrix* of the power system at the synchronous state. Note that the state variables in (5) characterize the deviations of the phase and frequencies deviate from the synchronous state $(\boldsymbol{\delta}^*, \mathbf{0})$. It is proven that if the weight $K_{i,j}\cos\delta_{ij}^*$ keeps positive for all the lines, the system is stable at the synchronous state $(\boldsymbol{\delta}^*, \mathbf{0})$ [36,37], which results in the security condition of the phase angle ability

$$\boldsymbol{\Theta} = \left\{\delta \in \mathbb{R}^n \middle|\ |\delta_{ij}| < \frac{\pi}{2}, \forall (i, j) \in \mathcal{E}\right\}. \tag{6}$$

Similarly, as in [28,29,32], we model the disturbance by a Brownian motion model, which serves as the input to a linearized system, and study the stochastic system

$$\mathrm{d}\boldsymbol{\delta}(t) = \boldsymbol{\omega}(t)\mathrm{d}t, \tag{7a}$$

$$\mathrm{d}\boldsymbol{\omega}(t) = -\mathbf{M}^{-1}\left(\mathbf{L}\boldsymbol{\delta}(t) + \mathbf{D}\boldsymbol{\omega}(t)\right)\mathrm{d}t + \mathbf{M}^{-1}\widetilde{\boldsymbol{B}}\mathrm{d}\mathbf{v}(t), \tag{7b}$$

with the state variable, system matrix and input matrix,

$$\boldsymbol{x} = \begin{bmatrix} \boldsymbol{\delta} \\ \boldsymbol{\omega} \end{bmatrix},\ \mathbf{A} = \begin{bmatrix} \mathbf{0} & \mathbf{I}_n \\ -\mathbf{M}^{-1}\mathbf{L} & -\mathbf{M}^{-1}\mathbf{D} \end{bmatrix},\ \mathbf{B} = \begin{bmatrix} \mathbf{0} \\ \mathbf{M}^{-1}\widetilde{\mathbf{B}} \end{bmatrix},$$

where $\widetilde{\mathbf{B}} = \mathrm{diag}(b_i) \in \mathbb{R}^{n\times n}$ with $b_i > 0$ being the strength of the disturbances of node i; $\mathbf{v}(t) = \mathrm{col}(\mathrm{v}_i(t)) \in \mathbb{R}^n$ where $\mathrm{v}_i(t)$ denotes a Brownian motion that results in Gaussian-distributed disturbance at each node. The noise components $\mathrm{v}_1, \mathrm{v}_2, \dots, \mathrm{v}_n$ are assumed to be independent. Here, we refer to $K_{i,j}$ as the *line capacity* of line e_k, which is also called the coupling strength between nodes, and refer to $w_{i,j} = K_{i,j}\cos\delta_{ij}^*$ as the *weight* of e_k. It is clear that the weights of the lines are influenced by the power flows at the synchronous state solved from (3) and the line capacities. Note that the weight depends on the line capacity in a non-linear way, i.e., increasing the line capacities of the lines, the phase differences δ_{ij}^* may decrease which further increases the weights of the lines.

Because the locations of the power generations including renewable energy are usually far from each other, the assumption of the independence of the disturbance $v_i(t)$ is reasonable in the model (7). The probability distribution of the state is Gaussian due to the linearity of the system (7). To reveal the dependence of the fluctuations on the system parameters, we focus on the variance matrix of the phase differences and the frequency in the invariant probability distribution of the linear stochastic system (7), which can be solved from a Lyapunov equation. For the invariant probability distribution of a Gaussian

stochastic process, we refer to [31,38], which are summarized in [28, Definition A.1]. The output matrix are set to

$$\mathbf{y} = \mathbf{C}\mathbf{x}, \quad \mathbf{y} = \begin{bmatrix} \mathbf{y}_\delta \\ \mathbf{y}_\omega \end{bmatrix}, \quad \mathbf{C} = \begin{bmatrix} \widetilde{\mathbf{C}}^\mathsf{T} & \mathbf{0} \\ \mathbf{0} & \mathbf{I}_n \end{bmatrix} \in \mathbb{R}^{(m+n)\times 2n}. \tag{8}$$

The vector $\mathbf{y}_\delta \in \mathbb{R}^m$ describes the phase differences in the m lines, and the vector $\mathbf{y}_\omega \in \mathbb{R}^n$ describes the frequencies at the n nodes. The matrix $\widetilde{\mathbf{C}} = (c_{i,k}) \in \mathbb{R}^{n\times m}$ denotes the incidence matrix of the graph $\mathcal{G}$. The variance matrix of the output is denoted by

$$\mathbf{Q}_y = \begin{bmatrix} \mathbf{Q}_\delta & \mathbf{Q}_{\delta\omega}^\mathsf{T} \\ \mathbf{Q}_{\delta\omega} & \mathbf{Q}_\omega \end{bmatrix} \in \mathbb{R}^{(m+n)\times(m+n)}, \tag{9}$$

with $\mathbf{Q}_\delta \in \mathbb{R}^m, \mathbf{Q}_{\delta\omega} \in \mathbb{R}^{n\times m}, \mathbf{Q}_\omega \in \mathbb{R}^{n\times n}$.

For comparison with the main result of this paper, we present the variance of the state in the invariant probability distribution of the linearized system of the Single-Machine Infinite Bus (SMIB) model, which is governed by the dynamics,

$$\dot{\delta} = \omega, \tag{10a}$$

$$\eta\dot{\omega} = P - d\omega - K\sin\delta. \tag{10b}$$

Assume there exists a synchronous state $(\arcsin(P/K), 0)$, the linear stochastic system of SMIB model corresponding to the system (7) is

$$\mathrm{d}\delta(t) = \omega(t)\mathrm{d}t, \tag{11a}$$

$$\mathrm{d}\omega(t) = -\eta^{-1}\big(l\delta(t) + d\omega(t)\big)\mathrm{d}t + \eta^{-1}\beta\mathrm{d}\mathbf{v}(t), \tag{11b}$$

where $l = K\cos\delta^* = \sqrt{K^2 - P^2}$. The system matrix and input matrix are

$$\mathbf{A} = \begin{bmatrix} 0 & 1 \\ -\eta^{-1}l & -\eta^{-1}d \end{bmatrix}, \quad \mathbf{B} = \begin{bmatrix} 0 \\ \eta^{-1}\beta \end{bmatrix}. \tag{12}$$

We set the output as $y = (\delta, \omega)^\mathsf{T}$. Because the matrix $\mathbf{A}$ with $l > 0$ is Hurwitz, the variance matrix of the state in the invariant probability distribution is solved from the following Lyapunov equation [31, Theorem 1.53,Lemma 1.5] and [38],

$$\mathbf{A}\mathbf{Q}_x + \mathbf{Q}_x\mathbf{A}^\mathsf{T} + \mathbf{B}\mathbf{B}^\mathsf{T} = \mathbf{0}.$$

We further obtain the variance matrix $\mathbf{Q}_y$ of the output

$$\mathbf{Q}_y = \mathbf{Q}_x = \begin{bmatrix} \frac{\beta^2}{2d\sqrt{K^2-P^2}} & 0 \\ 0 & \frac{\beta^2}{2\eta d} \end{bmatrix}. \tag{13}$$

From this formula, it is found that the variance of the phase fluctuations is independent of the generator inertia and the variance of the frequency is independent on the line capacity. The roles of the damping played on the suppression of the variance of the phase and the frequency are the same. Obviously, due to the simplicity of this model, the fluctuations in the power networks with multi-machines cannot be fully explored by this model.

The problem of the characterization of the asymptotic variance of the stochastic linear system (7) is described below.

Problem 3.3. Consider the stochastic linearized power system (7) with multi-machines. Deduce an analytic expression of the asymptotic variance of the output process $\mathbf{y}$ and display how this variance depends on the system parameters.

The theorem for the solution of Problem 3.3 makes use of the properties and the notations in the following lemma.

Lemma 3.4 ([28]). *Consider the matrix $\mathbf{L}$ and the diagonal matrix $\mathbf{M}$ in system (7). There exists an orthogonal matrix $\mathbf{U} \in \mathbb{R}^{n\times n}_{ortg}$ such that*

$$\mathbf{U}^\mathsf{T}\mathbf{M}^{-1/2}\mathbf{L}\mathbf{M}^{-1/2}\mathbf{U} = \boldsymbol{\Lambda}_n, \tag{14}$$

with $\boldsymbol{\Lambda}_n = diag(\lambda_i) \in \mathbb{R}^{n\times n}$ where $0 = \lambda_1 \le \lambda_2 \cdots \le \lambda_n$ being the eigenvalues of the matrix $\mathbf{M}^{-1/2}\mathbf{L}\mathbf{M}^{-1/2}$. Denote the eigenvectors corresponding to λ_i by $\boldsymbol{u}_i$ for $i = 1, \ldots, n$, then $\mathbf{U} = \begin{bmatrix} \mathbf{u}_1 & \mathbf{u}_2 & \cdots & \mathbf{u}_n \end{bmatrix}$ and $\boldsymbol{u}_1 = c^{-1}M^{1/2}\mathbf{1}_n$ where c is the L_2 norm of the vector $M^{1/2}\mathbf{1}_n$.

For the variance matrix in the invariant probability distribution of the stochastic system (7), we have the following theorem .

Theorem 3.5 ([28]). *Consider the stochastic system (7) with Assumption 3.2 and the notations of matrices in Lemma 3.4. Define matrices*

$$\begin{aligned} \mathbf{A}_e &= \begin{bmatrix} \mathbf{0} & \mathbf{I}_n \\ -\boldsymbol{\Lambda}_n & -\mathbf{U}^\mathsf{T}\mathbf{M}^{-1}\mathbf{D}\mathbf{U} \end{bmatrix} \in \mathbb{R}^{2n\times 2n}, \mathbf{B}_e = \begin{bmatrix} \mathbf{0} \\ \mathbf{U}^\mathsf{T}\mathbf{M}^{-\frac{1}{2}}\widetilde{\mathbf{B}} \end{bmatrix} \in \mathbb{R}^{2n\times n}, \\ \mathbf{C}_e &= \begin{bmatrix} \widetilde{\mathbf{C}}^\mathsf{T}\mathbf{M}^{-\frac{1}{2}}\mathbf{U} & \mathbf{0} \\ \mathbf{0} & \mathbf{M}^{-\frac{1}{2}}\mathbf{U} \end{bmatrix} \in \mathbb{R}^{(m+n)\times 2n}, \end{aligned} \tag{15}$$

which can be decomposed according to

$$\mathbf{A}_e = \begin{bmatrix} \mathbf{0} & \mathbf{A}_{12} \\ \mathbf{0} & \mathbf{A}_2 \end{bmatrix}, \quad \mathbf{B}_e = \begin{bmatrix} \mathbf{0} \\ \mathbf{B}_2 \end{bmatrix}, \quad \mathbf{C}_e = \begin{bmatrix} \mathbf{0} & \mathbf{C}_2 \end{bmatrix}, \tag{16}$$

where $\mathbf{A}_{12} \in \mathbb{R}^{1\times(2n-1)}$ and $\mathbf{A}_2 \in \mathbb{R}^{(2n-1)\times(2n-1)}$, $\mathbf{B}_2 \in \mathbb{R}^{(2n-1)\times 2n}$ and $\mathbf{C}_2$ is obtained by deleting the first column of the output matrix $\mathbf{C}_e$ so that

$$\mathbf{C}_2 = \begin{bmatrix} \widetilde{\mathbf{C}}^\mathsf{T}\mathbf{M}^{-1/2}\hat{\mathbf{U}} & \mathbf{0} \\ \mathbf{0} & \mathbf{M}^{-1/2}\mathbf{U} \end{bmatrix} \in \mathbb{R}^{(m+n)\times(2n-1)}, \tag{17}$$

with $\hat{\mathbf{U}} = \begin{bmatrix} \mathbf{u}_2 & \mathbf{u}_3 & \cdots & \mathbf{u}_n \end{bmatrix} \in \mathbb{R}^{n\times(n-1)}$. The variance matrix $\mathbf{Q}_y$ of the output $\mathbf{y}$ of the stochastic system (7) satisfies

$$\mathbf{Q}_y = \mathbf{C}_2\mathbf{Q}_x\mathbf{C}_2^\mathsf{T}, \tag{18}$$

where $\mathbf{Q}_x \in \mathbb{R}^{(2n-1)\times(2n-1)}$ is the unique solution of the following Lyapunov equation

$$\mathbf{A}_2\mathbf{Q}_x + \mathbf{Q}_x\mathbf{A}_2^\mathsf{T} + \mathbf{B}_2\mathbf{B}_2^\mathsf{T} = \mathbf{0}. \tag{19}$$

By assuming $b_i^2/d_i = b_j^2/d_j$ for $i, j \in \mathcal{V}$, the explicit formula the $\mathbf{Q}$ have been deduced in [28], from which the impact of the network topology is explored. However, the fluctuation propagation cannot be fully illustrated with this assumption.

To emphasize the effect of the inertia in the system (7), we also study the fluctuations in the stochastic process

$$\mathrm{d}\bar{\boldsymbol{\delta}}(t) = -\mathbf{D}^{-1}\mathbf{L}\bar{\boldsymbol{\delta}}(t)\mathrm{d}t + \mathbf{D}^{-1}\widetilde{\mathbf{B}}\mathrm{d}\boldsymbol{v}(t), \tag{20a}$$

$$\bar{\boldsymbol{y}}(t) = \widetilde{\mathbf{C}}^\mathsf{T}\bar{\boldsymbol{\delta}}(t), \tag{20b}$$

which is the linearization of the non-uniform Kuramoto model [32,39]. This system can also be obtained by setting $m_i = 0$ in the system (7) at all the nodes. Denote the matrix $\overline{\mathbf{U}} \in \mathbb{R}^{n\times n}$ such that

$$\overline{\mathbf{U}}^\mathsf{T}\mathbf{D}^{-1/2}\mathbf{L}\mathbf{D}^{-1/2}\overline{\mathbf{U}} = \overline{\boldsymbol{\Lambda}}_n, \tag{21}$$

where $\overline{\boldsymbol{\Lambda}}_n = (\bar{\lambda}_i) \in \mathbb{R}^{n\times n}$ with $\bar{\lambda}_i$ being the eigenvalue of the matrix $\mathbf{D}^{-1/2}\mathbf{L}\mathbf{D}^{-1/2}$. The matrix $\overline{\mathbf{U}}$ is further decomposed into the form $\overline{\mathbf{U}} = \begin{bmatrix} \bar{\mathbf{u}}_1 & \overline{\mathbf{U}}_2 \end{bmatrix}$.

For the model (20), the variance matrix of the phase angle difference is presented in the following theorem [32].

Theorem 3.6. *Consider the stochastic system (20) with a connected graph $\mathcal{G}$. The asymptotic variance of the output process $\bar{\mathbf{y}}$ can be computed by*

$$\overline{\mathbf{Q}}_\delta = \widetilde{\mathbf{C}}^\mathsf{T}\mathbf{D}^{-1/2}\overline{\mathbf{U}}_2\overline{\mathbf{Q}}_x\overline{\mathbf{U}}_2^\mathsf{T}\mathbf{D}^{-1/2}\widetilde{\mathbf{C}}, \tag{22}$$

where $\overline{\mathbf{U}}_2 = \begin{bmatrix} \bar{\mathbf{u}}_2 & \bar{\mathbf{u}}_3 & \ldots & \bar{\mathbf{u}}_n \end{bmatrix} \in \mathbb{R}^{n\times(n-1)}$ and $\overline{\mathbf{Q}}_x = (\bar{q}_{x_{i,j}}) \in \mathbb{R}^{(n-1)\times(n-1)}_{spd}$ is the unique solution of the Lyapunov equation,

$$\mathbf{0} = -\overline{\boldsymbol{\Lambda}}_{n-1}\overline{\mathbf{Q}}_x - \overline{\mathbf{Q}}_x\overline{\boldsymbol{\Lambda}}_{n-1} + \overline{\mathbf{U}}_2^\mathsf{T}\mathbf{D}^{-1/2}\widetilde{\mathbf{B}}\widetilde{\mathbf{B}}^\mathsf{T}\mathbf{D}^{-1/2}\overline{\mathbf{U}}_2, \tag{23}$$

with $\overline{\boldsymbol{\Lambda}}_{n-1} = diag(\bar{\lambda}_2, \bar{\lambda}_3, \ldots, \bar{\lambda}_n) \in \mathbb{R}^{(n-1)\times(n-1)}_{diag}$. In addition, the matrix $\overline{\mathbf{Q}}_x$ is solved from the Lyapunov equation such that for $i, j = 1, \cdots, n-1$,

$$\bar{q}_{x_{i,j}} = (\bar{\lambda}_{i+1} + \bar{\lambda}_{j+1})^{-1}\bar{\mathbf{u}}_{i+1}^\mathsf{T}\mathbf{D}^{-1/2}\widetilde{\mathbf{B}}\widetilde{\mathbf{B}}^\mathsf{T}\mathbf{D}^{-1/2}\bar{\mathbf{u}}_{j+1}, \tag{24}$$

and in particular, for $i = 1, \cdots, n-1$,

$$\bar{q}_{x_{i,i}} = \frac{1}{2}\bar{\lambda}_{i+1}^{-1}\bar{\mathbf{u}}_{i+1}^\mathsf{T}\mathbf{D}^{-1/2}\widetilde{\mathbf{B}}\widetilde{\mathbf{B}}^\mathsf{T}\mathbf{D}^{-1/2}\bar{\mathbf{u}}_{i+1}. \tag{25}$$

4. Main results

In this section, we present the main results of this paper. The reader may find the proofs of the results in Section 5. We focus on multi-machine systems (7). Based on the following assumption, we deduce the explicit formula of the variance matrix $\mathbf{Q}_y$.

Assumption 4.1. Consider the stochastic Gaussian system (7), assume the damping-inertia ratios d_i/m_i are uniform at all the nodes, i.e., for all $i \in \mathcal{V}$, $d_i/m_i = \alpha \in \mathbb{R}_+$.

This assumption allows us to derive explicit formulas of the variance matrix of the phase difference and the frequency, though in reality the damping-inertia ratio usually varies from machine to machine [40]. From the explicit formulas, new insights can be found on the propagation of the disturbances in the network. This assumption is often made in the calculation of the $\mathcal{H}_2$ norm to study the transient performance of the system when subjected to various disturbances [14–18] and in the investigation on the propagation of the disturbance with the metric of Rate of Change of Frequency(RoCoF) [21].

Following Theorem 3.5, we derive the following theorem.

Theorem 4.2. *Consider the invariant probability distribution of the system (7). Decompose the matrix $\mathbf{Q}_x$ defined in Theorem 3.5 into matrices,*

$$\mathbf{Q}_x = \begin{bmatrix} \mathbf{G} & \mathbf{S} \\ \mathbf{S}^\top & \mathbf{R} \end{bmatrix}, \tag{26}$$

where $\mathbf{G} = (g_{i,j}) \in \mathbb{R}^{(n-1)\times(n-1)}$ which satisfies $\mathbf{G} = \mathbf{G}^\top$, $\mathbf{S} = (s_{i,j}) \in \mathbb{R}^{(n-1)\times n}$ and $\mathbf{R} = (r_{i,j}) \in \mathbb{R}^{n\times n}$ which satisfies $\mathbf{R} = \mathbf{R}^\top$. The variance matrix $\mathbf{Q}_y$ with the form of block matrix in (9) satisfies

$$\mathbf{Q}_\delta = \widetilde{\mathbf{C}}^\top \mathbf{M}^{-1/2} \hat{\mathbf{U}} \mathbf{G} \hat{\mathbf{U}}^\top \mathbf{M}^{-1/2} \widetilde{\mathbf{C}}, \tag{27a}$$

$$\mathbf{Q}_\omega = \mathbf{M}^{-1/2} \mathbf{U} \mathbf{R} \mathbf{U}^\top \mathbf{M}^{-1/2}, \tag{27b}$$

$$\mathbf{Q}_{\delta\omega} = \mathbf{M}^{-1/2} \mathbf{U} \mathbf{S}^\top \hat{\mathbf{U}}^\top \mathbf{M}^{-1/2} \widetilde{\mathbf{C}}. \tag{27c}$$

Define

$$\rho_i = 2\alpha^2 + \lambda_i, \quad \chi_{i,j} = (\lambda_i - \lambda_j)^2 + 2\alpha^2(\lambda_j + \lambda_i).$$

If Assumption 4.1 holds, then $\mathbf{Q}_y$ can be solved from (27) with explicit formula of $\mathbf{Q}_x$ solved from the Lyapunov Eq. (19), where $\mathbf{S}$ satisfies for $i = 1, 2, \dots, n-1$,

$$s_{i,1} = \rho_{i+1}^{-1} \mathbf{u}_{i+1}^\top \mathbf{M}^{-1/2} \widetilde{\mathbf{B}}^2 \mathbf{M}^{-1/2} \mathbf{u}_1, \tag{28}$$

for $i, j = 2, 3, \dots, n$,

$$s_{i-1,j} = \frac{\lambda_i - \lambda_j}{\chi_{i,j}} \mathbf{u}_i^\top \mathbf{M}^{-1/2} \widetilde{\mathbf{B}}^2 \mathbf{M}^{-1/2} \mathbf{u}_j. \tag{29}$$

$\mathbf{G}$ satisfies for $i, j = 2, 3, \dots, n$,

$$g_{i-1,j-1} = \frac{2\alpha}{\chi_{i,j}} \mathbf{u}_i^\top \mathbf{M}^{-1/2} \widetilde{\mathbf{B}}^2 \mathbf{M}^{-1/2} \mathbf{u}_j. \tag{30}$$

$\mathbf{R}$ satisfies

$$r_{1,1} = \frac{1}{2\alpha} \mathbf{u}_1^\top \mathbf{M}^{-1/2} \widetilde{\mathbf{B}}^2 \mathbf{M}^{-1/2} \mathbf{u}_1, \tag{31}$$

for $i, j = 1, 2, \dots, n$, with $(i, j) \neq (1, 1)$,

$$r_{i,j} = \frac{\alpha(\lambda_i + \lambda_j)}{\chi_{i,j}} \mathbf{u}_i^\top \mathbf{M}^{-1/2} \widetilde{\mathbf{B}}^2 \mathbf{M}^{-1/2} \mathbf{u}_j. \tag{32}$$

Here $\widetilde{\mathbf{B}}^2 = \widetilde{\mathbf{B}}\widetilde{\mathbf{B}}^\top$ because $\widetilde{\mathbf{B}}$ is a diagonal matrix.

See Section 5 for the proof of this theorem. Following this theorem, the *Superposition Principle* can be used to describe the impact of the disturbances. *This property demonstrates that the fluctuations in the system caused by the disturbance at a node can never be balanced by the disturbances at the other nodes.*

To reveal the influences of the system parameters on the fluctuations more explicitly, we further make an assumption.

Assumption 4.3. Assume that the inertia and the damping of the synchronous machines are all identical in the system, i.e., $\mathbf{M} = \eta \mathbf{I}_n$ and $\mathbf{D} = d\mathbf{I}_n$, which leads to $\alpha = d/\eta$.

Clearly, this assumption is more restrictive than Assumption 4.1, with which we obtain the following corollary for the trace of the variance matrix of the frequency (31).

Corollary 4.4. *Consider the system (7). If Assumption 4.3 holds, then the variance matrix of the frequency satisfies*

$$tr(\mathbf{Q}_\omega) = \frac{1}{2d\eta} tr(\widetilde{\mathbf{B}}^2).$$

The proof follows immediately from $\mathrm{tr}(\mathbf{R}) = \frac{1}{2\alpha\eta}\mathrm{tr}(\widetilde{\mathbf{B}}^2)$ with the fact that pre- and post-multiplication of the matrix $\widetilde{\mathbf{B}}^2$ by the orthogonal matrix $\mathbf{U}$ according to $\mathbf{U}\widetilde{\mathbf{B}}^2\mathbf{U}^\top$ will not change the trace of this matrix. If Assumption 4.3 is applied, this formula can also be obtained from the result of [9, Theorem 3] deduced from the corresponding $\mathcal{H}_2$ norm.

Following from this corollary, it is found that adding new nodes without any disturbances will not change the total amount of fluctuations in the network if Assumption 4.3 is satisfied. It is shown that the trace of the variance matrix of the frequency is independent on the network topology. However, it will be shown in the next section that the variance of the frequency at each node depend on the network topology.

Based on Assumption 4.3 and Theorem 4.2, we investigate the propagation of the disturbance in two types of special graphs, i.e., complete graphs and star graphs. For simplicity, we further make an assumption on the weight of the lines as below.

Assumption 4.5. Assume the weights of the lines in the graph are all identical, i.e., $K_{i,j}\cos\delta_{ij}^* = \gamma$ for $(i, j) \in \mathcal{E}$.

This assumption is practical for the power networks with identical line capacities and small phase differences at the synchronous state., i.e., $\delta_i^* \approx \delta_j^*$ for all $(i, j) \in \mathcal{E}$. Together with the analytic formulas of the eigenvalues of the Laplacian matrices of complete graphs and star graphs in Appendix A.1, this allows us to derive the explicit formulas of the variance matrix of the phase differences and the frequencies in the power networks with complete graphs and star graphs. In these explicit formulas, the eigenvalues will not emerge explicitly, which enables us to reveal the impact of the system parameters independent of the eigenvalues, such as the impacts of the size of network, the line capacity, the inertia and damping of the synchronous machines on the fluctuation propagation in the network.

4.1. Complete graphs

For a power systems with a complete graph, it yields the following proposition from Theorem 4.2 and Eq. (A.1) in Appendix.

Proposition 4.6. *Consider the system (7) with a complete graph. If Assumptions 4.3 and 4.5 hold, then the variance of the frequency at node i for $i = 1, 2, \dots, n$ satisfies*

$$q_{\omega_{i,i}} = \Big[\frac{1}{2d\eta} - \frac{\gamma(n-1)}{dn(2d^2 + \gamma\eta n)}\Big] b_i^2 + \frac{\gamma(tr(\widetilde{\mathbf{B}}^2) - b_i^2)}{dn\left(2d^2 + \gamma\eta n\right)}, \tag{33}$$

and the variance matrix $\boldsymbol{Q}_\delta$ of the phase difference satisfies

$$\mathbf{Q}_\delta = \frac{1}{2d\gamma n} \widetilde{\mathbf{C}}^\top \widetilde{\mathbf{B}}^2 \widetilde{\mathbf{C}}. \tag{34}$$

In particular, for the line e_k connecting node i and j, the variance of the phase difference in this line is

$$q_{\delta_{k,k}} = \frac{1}{2d\gamma n}(b_i^2 + b_j^2), \tag{35}$$

and the trace of $\mathbf{Q}_\delta$ satisfies

$$tr(\mathbf{Q}_\delta) = \frac{n-1}{2d\gamma n} tr(\widetilde{\mathbf{B}}^2). \tag{36}$$

Table 1
The setting of the parameters for plotting Figs. 2 and 3.

Parameters	Fig. 2				Fig. 3			
	(a)	(b)	(c)	(d)	(a)	(b)	(c)	(d)
γ	10	10	–	10	10	10	–	10
η	0.5	–	0.02	0.02	0.5	–	0.01	0.1
d	–	0.3	1.2	1.5	–	0.1	1.2	0.1
b_2	0.04	0.04	0.04	0.05	0.8	0.8	1.5	1
n	20	20	30	–	20	10	50	–

The next corollary of Proposition 4.6 explains the finding on the propagation of the fluctuations from a node to the others in details.

Corollary 4.7. *Consider the system (7) with a complete graph. If Assumptions 4.3 and 4.5 holds, and $b_i \neq 0$ and $b_j = 0$ for all j with $j \neq i$, then*

$$q_{\omega_{i,i}} = \frac{b_i^2}{2d\eta} - \frac{(n-1)\gamma b_i^2}{dn(2d^2+\gamma\eta n)}, \tag{37}$$

$$q_{\omega_{j,j}} = \frac{\gamma b_i^2}{dn\left(2d^2+\gamma\eta n\right)}, \text{ for } j \neq i, \tag{38}$$

and the variances of the phase differences satisfy

$$q_{\delta_{k,k}} = \begin{cases} \frac{b_i^2}{2d\gamma n}, & \text{if line } e_k \text{ is connected to node } i, \\ 0, & \text{else.} \end{cases} \tag{39}$$

For comparison, the asymptotic matrix of the phase differences in the model (20) is presented in the following proposition with proof in Section 5.

Proposition 4.8. *Consider the system (20) with a complete graph. Assume $\mathbf{D} = d\mathbf{I}$ and Assumption 4.5 holds, then the variances of the phase differences satisfy*

$$\overline{\mathbf{Q}}_\delta = \frac{1}{2d\gamma n}\widetilde{\mathbf{C}}^{\mathsf{T}}\widetilde{\mathbf{B}}^2\widetilde{\mathbf{C}}, \tag{40}$$

with

$$\overline{q}_{\delta_{k,k}} = \frac{1}{2d\gamma n}(b_i^2+b_j^2), \text{ for } k = 1,\dots,m. \tag{41}$$

To verify the correctness of these analytical formulas in Corollary 4.7, we use Matlab to compute the variances numerically from (18) and (19) in the complete graph with $b_2 \neq 0$ and $b_j = 0$ for $j \neq 2$ and indices of the nodes and lines defined in Definition 2.2(i). In order to satisfy Assumption 4.5, we set $P_i = 0$ for all the nodes and $K_{ij} = K$ for all the lines in the system (2), which leads to $\delta_i^* - \delta_j^* = 0$ at the synchronous state and the line weight $\gamma = K\cos\delta_{ij}^* = K$. The setting of the parameters for plotting these figures are shown in Table 1. It is shown in Fig. 2 and Fig. 3 that the analytical solution and the numerical solution of the variances are all identical.

Based on Corollary 4.7 and Proposition 4.8, we get the following findings on the variance of the frequency and the phase differences in the stochastic system (20) with the complete graph.

(a) On the variance of the frequency in the complete graph. As either the inertia η or the damping d of the synchronous machines increases, the variance of the frequencies at all the nodes decrease. This statement is well known to experts in the field and will not be discussed further. There are two terms in the right hand side of (37), in which the first term is the variance of the fluctuations introduced by the disturbance at node i and the second term measures the fluctuations propagated from node i to all the other nodes. Thus, we only need to analyze the dependence of the variance of the frequency at node i on the weight of the lines and the network size.

First, we describe the impact of the line weights. On contrary to the case of SMIB model, the weights of the lines play roles on the variance of the frequency. The derivative of the variance with respect to γ satisfy

$$\frac{\partial q_{\omega_{i,i}}}{\partial\gamma} = \frac{2d(1-n)b_i^2}{n(2d^2+\gamma\eta n)^2} < 0, \quad \frac{\partial q_{\omega_{j,j}}}{\partial\gamma} = \frac{2db_i^2}{n(2d^2+\gamma\eta n)^2} > 0.$$

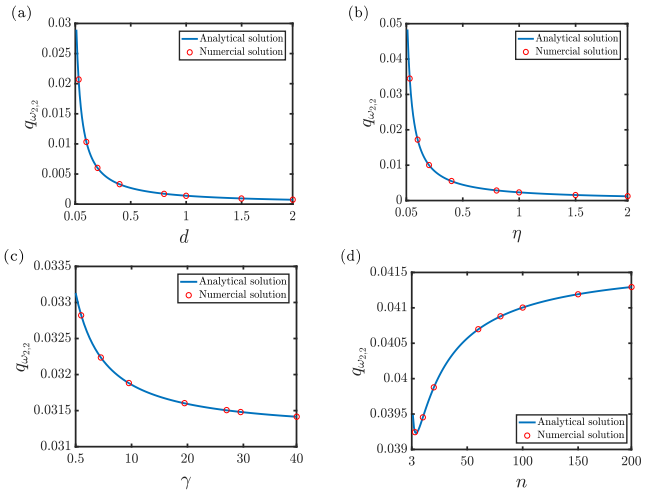

Fig. 2. The dependence of the variance $q_{\omega_{2,2}}$ on the system parameters in the complete graph with $b_2 \neq 0$ and $b_j = 0$ for $j \neq 2$ and indices of the nodes and lines defined in Definition 2.2(i).

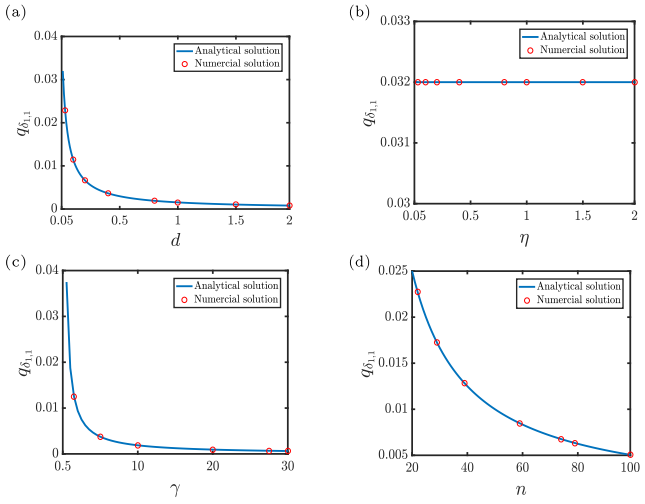

Fig. 3. The relationship for the variance $q_{\delta_{1,1}}$ for line $(1,2)$ in the complete graph with $b_2 \neq 0$ and $b_j = 0$ for $j \neq 2$ and indices of the nodes and lines defined in Definition 2.2(i).

This indicates that, as the line weights increase, the frequency variance at the source node of the disturbance decreases while those at the other nodes increase. Thus, increasing the line capacities, which increases the line weights, will accelerate the propagation of the fluctuation from the source node to the other nodes. However, there exists a lower bound for the variance of the frequency at nodes and an upper bound for the variance of the frequency at the other nodes, which are the limits of the variance as γ goes to infinity respectively,

$$\lim_{\gamma\to\infty} q_{\omega_{i,i}} = \frac{1}{2d\eta}b_i^2 - \frac{n-1}{d\eta n^2}b_i^2, \quad \text{and} \quad \lim_{\gamma\to\infty} q_{\omega_{j,j}} = \frac{1}{d\eta n^2}b_i^2.$$

This indicates that the acceleration of the propagation of the frequency fluctuations by increasing the line capacities is limited.

Second, we focus on the impact of the network size. From (37), it yields

$$\lim_{n\to\infty} q_{\omega_{i,i}} = \frac{b_i^2}{2d\eta}.$$

Clearly, this limit equals to the value of the frequency variance presented in (13) for the SMIB model. This indicates that the network becomes an infinite bus for node i when the size is sufficiently large. If the size of the network is large, then it holds

$$\frac{1}{2d\eta}b_i^2 \gg \frac{\gamma(n-1)}{dn(2d^2+\gamma\eta n)}b_i^2,$$

which demonstrates that the disturbance impacts the local node most. In addition, the derivative of the variances with respect to n satisfies

$$\frac{\partial q_{\omega_{i,i}}}{\partial n} = \frac{\gamma(\gamma\eta n^2 - 2\gamma\eta n - 2d^2)}{d(2d^2 n + \gamma\eta n^2)^2}b_i^2,$$
$$\frac{\partial q_{\omega_{j,j}}}{\partial n} = \frac{-\gamma(2d^2+2\gamma\eta n)}{d(2d^2 n + \gamma\eta n^2)^2}b_i^2 < 0.$$

It is found that if $n > n_c$ with $n_c = \lfloor 1 + \sqrt{1+\frac{2d^2}{\gamma\eta}} \rfloor$ defined as a critical value of the network size, then

$$\frac{\partial q_{\omega_{i,i}}}{\partial n} > 0.$$

This indicates that the variance of the frequency at node i increases as the size of the network increases. This trend is shown in Fig. 2(d) for the graph with $b_2 \neq 0$ and $b_j = 0$ for $j \neq 2$.

It is found that when $n > n_c$, increasing the size of the network have a negative impact on suppressing the frequency variance at node i. In other words, a newly added node to the network prevents the propagation of the fluctuations from the disturbance's source node to the other nodes though it helps to dissipate the fluctuations. In addition, for any $n \geq 2$, it holds

$$q_{\omega_{i,i}} \geq \left(\frac{1}{2d\eta} - \frac{\gamma}{d(\sqrt{\gamma\eta}+\sqrt{\gamma\eta+2d^2})^2}\right)b_i^2,$$

which shows the lower bound of the variance of the frequency at node i.

(b) On the variance of the phase difference in the complete graph. The roles of the damping coefficient d, the line weight γ, the graph size n can be clearly seen from the formula (35). Because the inertia η is absent in this formula, the variance is independent on the inertia of the node. Due to this independence, the variance matrix of the phase difference in the system (7) and the system (20) are equal, i.e., $\overline{\mathbf{Q}}_\delta = \mathbf{Q}_\delta$, which is verified by the formula (34) and (40). It is surprisingly found that the variance only depends on the disturbance from the node i and j while it is independent on the disturbances from all the other nodes. In addition, as the size of the network increases, the variances of the phase differences in the lines connecting node i decrease. This is because as the size of the complete graph increases, the lines connecting node i also increases, which dissipate the fluctuation from node i.

4.2. Star graphs

In this subsection, we study the variance matrices in the systems with star graphs. Based on Theorem 4.2 and Eq. (A.2) in the Appendix, we obtain the following result.

Proposition 4.9. *Consider the system (7) with a star graph where the indices of the nodes and lines are defined as in Definition 2.2(ii). If the Assumptions 4.3 and 4.5 both holds, then the variance $\mathbf{Q}_\omega$ of the frequency satisfies*

$$q_{\omega_{1,1}} = \left[\frac{1}{2d\eta} - \frac{\gamma(n-1)}{dn(2d^2+\gamma\eta n)}\right]b_1^2 + \frac{\gamma(tr(\widetilde{\mathbf{B}}^2)-b_1^2)}{dn\left(2d^2+\gamma\eta n\right)}, \tag{42}$$

and for $i = 2, 3, \ldots, n$,

$$\begin{aligned} q_{\omega_{i,i}} =& \frac{\gamma b_1^2}{dn\left(2d^2+\gamma\eta n\right)} + \frac{b_i^2}{2d\eta} - \frac{\gamma b_i^2}{dn(2d^2+\gamma\eta n)} \\ &- \frac{\gamma(n-2)b_i^2}{dn(2d^2(n+1)+\gamma\eta(n-1)^2)} - \frac{\gamma^2\eta(n-2)b_i^2}{dn(2d^2+\gamma\eta)(2d^2+\gamma\eta n)} \\ &+ \frac{\gamma(tr(\widetilde{\mathbf{B}}^2)-b_i^2-b_1^2)}{dn(2d^2(1+n)+\gamma\eta(n-1)^2)} + \frac{\gamma^2\eta(tr(\widetilde{\mathbf{B}}^2)-b_i^2-b_1^2)}{dn(2d^2+\gamma\eta)(2d^2+\gamma\eta n)}, \end{aligned}$$

and the variance matrix $\mathbf{Q}_\delta$ of the phase differences satisfies for $k \neq q$,

$$\begin{aligned} q_{\delta_{k,q}} =& \frac{2d^2(n+1)+\gamma\eta(n-1)^2}{2dn\gamma(n(2d^2(1+n)+\gamma\eta(n-1)^2)}b_1^2 \\ &+ \frac{-2d^2(n-1)+\gamma\eta(2n-n^2+1)}{2dn\gamma(n(2d^2(1+n)+\gamma\eta(n-1)^2)}b_{k+1}^2 + \frac{-2d^2(n-1)+\gamma\eta(2n-n^2+1)}{2dn\gamma(n(2d^2(1+n)+\gamma\eta(n-1)^2)}b_{q+1}^2 \\ &+ \frac{(2d^2+\gamma\eta(n+1))\left(tr(\widetilde{\mathbf{B}}^2)-b_{k+1}^2-b_{q+1}^2-b_1^2\right)}{2dn\gamma(n(2d^2(1+n)+\gamma\eta(n-1)^2)}, \end{aligned}$$

and for $k = 1, \ldots, m$,

$$\begin{aligned} q_{\delta_{k,k}} =& \frac{b_1^2}{2dn\gamma} + \left(\frac{n-1}{2dn\gamma} - \frac{(n-2)(2d^2+\gamma\eta(n+1))}{2dn\gamma(n(2d^2(1+n)+\gamma\eta(n-1)^2)}\right)b_{k+1}^2 \\ &+ \frac{(2d^2+\gamma\eta(n+1))\left(tr(\widetilde{\mathbf{B}}^2)-b_{k+1}^2-b_1^2\right)}{2dn\gamma(n(2d^2(1+n)+\gamma\eta(n-1)^2)}, \end{aligned} \tag{43}$$

and the trace of $\mathbf{Q}_\delta$ satisfies

$$tr(\mathbf{Q}_\delta) = \frac{n-1}{2dn\gamma}tr(\widetilde{\mathbf{B}}^2). \tag{44}$$

See the proof of this proposition in Section 5. With these explicit formulas, we investigate the propagation of the disturbances in the star graphs. We first focus on the graphs with a disturbance at the root node and then on the networks with a disturbance at a non-root node.

Corollary 4.10. *Consider the system (7) with a star graph where the indices of the nodes and lines are defined as in Definition 2.2(ii). If Assumptions 4.3 and 4.5 hold and there are disturbances at the root node $i = 1$ and no disturbances at all the other nodes, i.e., $b_1 \neq 0$ and $b_i = 0$ for $i = 2, \ldots, n$, then the variances matrix $\mathbf{Q}_\omega$ of the frequencies satisfies*

$$q_{\omega_{1,1}} = \left[\frac{1}{2d\eta} - \frac{\gamma(n-1)}{dn(2d^2+\gamma\eta n)}\right]b_1^2,$$

and for the other nodes,

$$q_{\omega_{i,i}} = \frac{\gamma}{dn\left(2d^2+\gamma\eta n\right)}b_1^2,\ i = 2, \ldots, n,$$

and the variances $\mathbf{Q}_\delta$ of the phase differences satisfy

$$q_{\delta_{k,k}} = \frac{1}{2dn\gamma}b_1^2,\ k = 1, \ldots, n-1.$$

It is clearly seen in this corollary that the formulas are all the same to the ones in Corollary 4.7 when $i = 1$. This demonstrates that when there are disturbance at the root node $i = 1$ only in the star graph, the dependence of the variances of the frequency and the phase difference on the system parameters, i.e., the damping and inertia of synchronous machines, the size of the network and the weights of the lines, are total the same as in the complete graph, which will not be explained again.

If the disturbances occurs at the non-root node, we obtain the following corollary.

Corollary 4.11. *Consider the system (7) with a star graph where the indices of the nodes and lines are defined as in Definition 2.2(ii). If Assumptions 4.3 and 4.5 hold and there are disturbances at node $i = 2$ and no disturbances at all the other nodes, i.e., $b_2 \neq 0$ and $b_1 = 0$ and $b_i = 0$ for $i = 3, \ldots, n$, then the variances matrix $\mathbf{Q}_\omega$ of the frequencies satisfies*

$$q_{\omega_{1,1}} = \frac{\gamma}{dn(2d^2+\gamma\eta n)}b_2^2, \tag{45}$$

Table 2
The setting of the parameters for plotting Figs. 4–6.

Parameters	Fig. 4				Fig. 5				Fig. 6			
	(a)	(b)	(c)	(d)	(a)	(b)	(c)	(d)	(a)	(b)	(c)	(d)
γ	10	10	–	10	10	10	–	10	10	10	–	10
η	0.5	–	0.02	0.02	0.5	–	0.01	0.1	0.5	–	0.01	0.1
d	–	0.3	1.2	1.5	–	0.2	1.2	0.4	–	0.2	1.2	0.4
b_2	0.04	0.04	0.04	0.05	0.2	0.5	0.5	0.5	0.2	0.5	0.5	0.5
n	20	20	30	–	20	10	50	–	20	10	50	–

$$q_{\omega_{2,2}} = \frac{b_2^2}{2d\eta} - \frac{\gamma b_2^2}{dn(2d^2+\gamma\eta n)} - \frac{\gamma(n-2)b_2^2}{dn(2d^2(n+1)+\gamma\eta(n-1)^2)} - \frac{\gamma^2\eta(n-2)b_2^2}{dn(2d^2+\gamma\eta)(2d^2+\gamma\eta n)}, \tag{46}$$

and for $i = 3, \dots, n$,

$$q_{\omega_{i,i}} = \frac{\gamma b_2^2}{dn(2d^2(1+n)+\gamma\eta(n-1)^2)} + \frac{\gamma^2\eta b_2^2}{dn(2d^2+\gamma\eta)(2d^2+\gamma\eta n)}, \tag{47}$$

the variances matrix $\mathbf{Q}_\delta$ *of the phase differences satisfies,*

$$q_{\delta_{1,1}} = \left(\frac{n-1}{2d\gamma n} - \frac{(n-2)(2d^2+\gamma\eta(n+1))}{2d\gamma n(2d^2(1+n)+\gamma\eta(n-1)^2)}\right)b_2^2, \tag{48}$$

$$q_{\delta_{k,k}} = \frac{2d^2+\gamma\eta(n+1)}{2d\gamma n(2d^2(1+n)+\gamma\eta(n-1)^2)}b_2^2. \tag{49}$$

To emphasize the impact of the inertia, we deduce the variance matrix of the system (20) with a star graph.

Proposition 4.12. *Consider the system (20) with a star graph where the indices of the nodes and lines are defined as in Definition 2.2(ii). Assume* $\mathbf{D} = d\mathbf{I}_n$ *and Assumption 4.5 hold, then the matrix* $\overline{\mathbf{Q}}_\delta$ *satisfies*

$$\overline{q}_{\delta_{k,q}} = \frac{b_1^2}{2d\gamma n} + \frac{(1-n)(b_{k+1}^2+b_{q+1}^2)}{2d\gamma n(1+n)} + \frac{1}{2d\gamma n(1+n)}\left(tr\left(\widetilde{\mathbf{B}}^2\right) - b_{k+1}^2 - b_{q+1}^2 - b_1^2\right), \tag{50}$$

and

$$\overline{q}_{\delta_{k,k}} = \frac{1}{2d\gamma n}b_1^2 + \frac{n^2-n+1}{2d\gamma n(1+n)}b_{k+1}^2 + \frac{1}{2d\gamma n(1+n)}\left(tr\left(\widetilde{\mathbf{B}}^2\right) - b_{k+1}^2 - b_1^2\right). \tag{51}$$

Similar as for the complete graphs, we verify the correctness of the analytical formulas in Corollary 4.11 by comparing the analytical solution with the numerical solution which is computed by Matlab from (18) and (19) in the star graph with $b_2 \neq 0$ and $b_i = 0$ for $i \neq 2$ and indices of the nodes and lines defined in Definition 2.2(ii). In order to satisfy Assumption 4.5, we set $P_i = 0$ for all the nodes and $K_{ij} = K$ for all the lines in system (2), which leads to $\gamma = K\cos\delta_{ij}^* = K$. The setting of the parameters for plotting these figures are shown in Table 2. The results of these comparison are shown in Figs. 4–6, which demonstrate that these explicit formulas are all correct.

Based on Corollary 4.11, we analyze the dependence of the variances of the phase difference and the frequency on the system parameters.

(a) On the variance of the frequency in the star graph. As in the complete graph, the roles of the inertia η and the damping d of the synchronous machines are clear, which will not be discussed again. Here, we focus on the impacts of the weights of lines and the network size. There are four terms in the right hand of (46), i.e., the first term is the total amount of fluctuations caused by the disturbance at node $i = 2$, which equals to the trace of the matrix $\mathbf{Q}_\omega$, the absolute value of the second term measures the fluctuations propagating to the root node $i = 1$ and the absolute value of the sum of the third and the fourth term measure the fluctuations propagating to the other $n-2$ nodes.

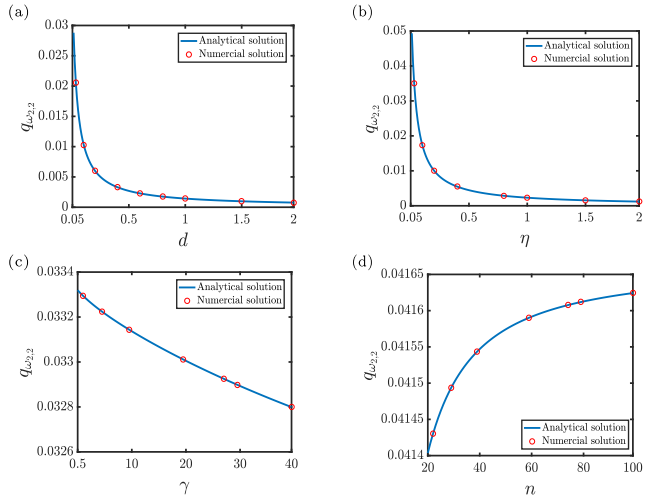

Fig. 4. The dependence of the variance $q_{\omega_{2,2}}$ on the system parameters in the star graph with $b_2 \neq 0$ and $b_i = 0$ for $i \neq 2$ and indices of the nodes and lines defined in Definition 2.2(ii).

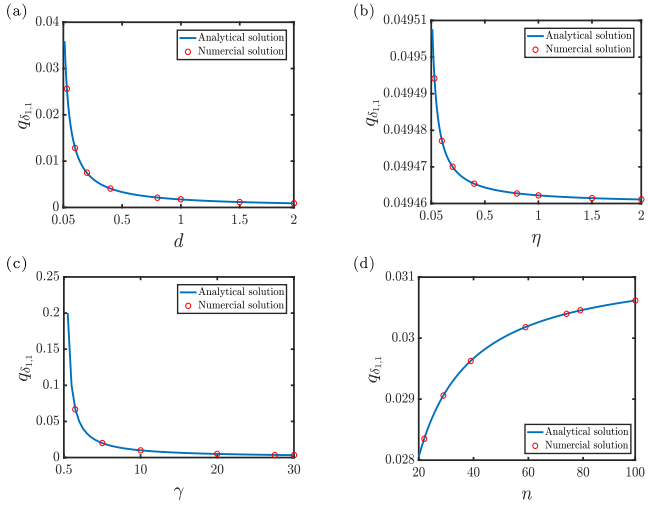

Fig. 5. The dependence of variance $q_{\delta_{1,1}}$ for line $(1,2)$ on the system parameters in the star graph with $b_2 \neq 0$ and $b_i = 0$ for $i \neq 2$ and indices of the nodes and lines defined in Definition 2.2(ii).

First, on the influences of the weights of the lines, it yields from (46) that

$$\frac{\partial q_{\omega_{2,2}}}{\partial\gamma} = -\frac{2db_2^2}{n(2d^2+\gamma\eta n)^2} - \frac{2d(n+1)(n-2)b_2^2}{n(2d^2(n+1)+\eta\gamma(n-1)^2)^2} - \frac{2d\gamma\eta(4+\gamma\eta(n+1))(n-2)b_2^2}{n(2d^2+\gamma\eta)^2(2d^2+\gamma\eta n)^2} < 0,$$

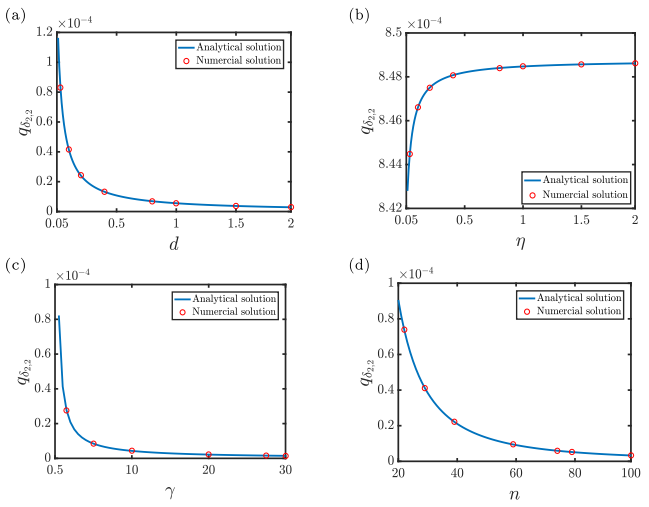

Fig. 6. The dependence of variance $q_{\delta_{2,2}}$ for line $(1,3)$ on the system parameters in the star graph with $b_2 \neq 0$ and $b_i = 0$ for $i \neq 2$ and indices of the nodes and lines defined in Definition 2.2(ii).

which indicates that as the weight of the lines increases, the variance of the frequency at the node with disturbance decrease. Thus, increasing the line capacity will accelerate the propagation of the fluctuations in the graph. The lower bound of this variance is obtained as the limit as γ increases to the infinity,

$$\lim_{\gamma\to\infty} q_{\omega_{2,2}} = \frac{b_2^2}{2d\eta} - \frac{b_2^2}{d\eta}\left(\frac{1}{n} - \frac{1}{n^2(n-1)^2}\right).$$

This indicates again that the acceleration of the propagation of the frequency fluctuations by increasing the line capacities is limited.

Second, for the impact of the network size, we get from (46) that for $n \geq 2$,

$$\frac{\partial q_{\omega_{2,2}}}{\partial n} = \frac{2\gamma b_2^2(d^2+\gamma\eta n)}{dn^2(2d^2+\gamma\eta n)^2} - \frac{\gamma^2\eta b_2^2(4d^2+\gamma\eta n(4-n))}{dn^2(2d^2+\gamma\eta)(2d^2+\gamma\eta n)^2} + \frac{2\gamma b_2^2(d^2(n^2-4n-2)+\gamma\eta(n-1)(n^2-3n+1))}{dn^2(2d^2(n+1)+\gamma\eta(n-1)^2)^2} > 0,$$

and

$$\lim_{n\to\infty} q_{\omega_{2,2}} = \frac{b_2^2}{2d\eta}.$$

The dependence of the variance $q_{\omega_{2,2}}$ on the size n is shown in Fig. 4(d). Because the derivative of $q_{\omega_{2,2}}$ with respect to n is positive, the variance of the frequency at node $i = 2$ increases at the size of the network increases. Note that the critical size n_c in the complete graph does not exist in the star graph. Clearly, as the size n increases to infinity, the variance $q_{\omega_{2,2}}$ converges to the value of the synchronous machine in the SMIB model. ***This shows that for a sufficiently large size graph, the graph plays roles as an infinite bus on each synchronous machine connecting this graph.***

(b) On the variance of the phase difference in the star graph. The impacts of the line weight γ and the damping coefficient d on the variance of the phase difference, which can be obtained from (48) and (49) directly, will not be discussed here. We focus on the impact of the size n and the inertia η.

A new finding is that the variance also depends on the inertia in the star graph. By (48) and (49), we obtain

$$\frac{\partial q_{\delta_{1,1}}}{\partial \eta} = -\frac{4(n-2)db_2^2}{[2d^2(n+1)+\gamma\eta(n-1)^2]^2} \leq 0,$$
$$\frac{\partial q_{\delta_{k,k}}}{\partial \eta} = \frac{4db_2^2}{[2d^2(n+1)+\gamma\eta(n-1)^2]^2} > 0.$$

From the perspective of the fluctuations of the phase difference, this demonstrates that increasing the inertia of the system, the amount of the fluctuations of the system propagating from the node $n = 2$ to the other non-root nodes increase. This trend can be seen in Fig. 5(b) and Fig. 6(b). This is different from the findings in the network with uniform damping-disturbance ratio, where the inertia has no impact on the variances of the phase differences [28]. However, it is obtained that

$$\lim_{\eta\to 0^+} q_{\delta_{1,1}} = \left(\frac{n-1}{2d\gamma n} - \frac{n-2}{2d\gamma n(n+1)}\right)b_2^2,$$
$$\lim_{\eta\to 0^+} q_{\delta_{k,k}} = \frac{1}{2d\gamma n(n+1)}b_2^2.$$

This indicates the fluctuation suppression of the phase differences by increasing the inertia is limited.

Regarding to the influence of the network size n, we derive

$$\frac{\partial q_{\delta_{1,1}}}{\partial n} = \frac{4d^4(2n^2-2n-1)+4d^2\gamma\eta(2n^3-6n^2+n-1)}{2d\gamma n^2(2d^2(1+n)+\gamma\eta(n-1)^2)^2} + \frac{\gamma^2\eta^2(n-1)(2n^3-4n^2-3n+1)}{2d\gamma n^2(2d^2(1+n)+\gamma\eta(n-1)^2)^2}b_2^2 > 0,$$
$$\frac{\partial q_{\delta_{kk}}}{\partial n} = -\frac{4d^4(1+2n)+4d^2\gamma\eta(2n^2-n+1)}{2d\gamma n^2(2d^2(1+n)+\gamma\eta(n-1)^2)^2}b_2^2 - \frac{\gamma^2\eta^2(n-1)(2n^2+3n-1)}{2d\gamma n^2(2d^2(1+n)+\gamma\eta(n-1)^2)^2}b_2^2 < 0.$$

This indicates that in the star graph the fluctuations the line connecting to the source node of the disturbance will increase as the graph size increases, while the fluctuations in other lines will decreases. These trends can also be observed in Figs. 5(d) and 6(d).

Comparing the formulas of $\mathbf{Q}_\delta$ in Proposition 4.9 to that of $\overline{\mathbf{Q}}_\delta$ in Proposition 4.12, it is found that

$$\lim_{\eta\to 0^+} \mathbf{Q}_\delta = \overline{\mathbf{Q}}_\delta,$$

where $\eta \to 0^+$ means that the inertia goes to zero. ***This property demonstrates that the variance of the phase difference in a power system with very small inertia can be estimated by that in the non-uniform Kuramoto model of a star graph.***

5. The proofs

In (16), $\mathbf{A}_2$ and $\mathbf{B}_2$ are further decomposed as,

$$\mathbf{A}_2 = \begin{bmatrix} \mathbf{0} & \mathbf{A}_{22} \\ \mathbf{A}_{23} & \mathbf{A}_{24} \end{bmatrix}, \quad \mathbf{B}_2 = \begin{bmatrix} \mathbf{0} \\ \mathbf{B}_{22} \end{bmatrix}, \tag{52}$$

where

$$\mathbf{A}_{22} = \begin{bmatrix} \mathbf{0} & \mathbf{I}_{n-1} \end{bmatrix} \in \mathbb{R}^{(n-1)\times n}, \quad \mathbf{A}_{23}^\top = \begin{bmatrix} \mathbf{0} & -\mathbf{\Lambda}_{n-1} \end{bmatrix} \in \mathbb{R}^{(n-1)\times n}, \tag{53a}$$
$$\mathbf{A}_{24} = -\mathbf{U}^\top\mathbf{M}^{-1}\mathbf{D}\mathbf{U} \in \mathbb{R}^{n\times n}, \quad \mathbf{B}_{22} = \mathbf{U}^\top\mathbf{M}^{-1/2}\widetilde{\mathbf{B}} \in \mathbb{R}^{n\times n}. \tag{53b}$$

Here, $\mathbf{\Lambda}_{n-1} = \mathrm{diag}(\lambda_i, i = 2,\dots,n) \in \mathbb{R}^{(n-1)\times(n-1)}$ is obtained by removing the first column and the first row of the diagonal matrix $\mathbf{\Lambda}_n$.

Proof of Theorem 4.2. With the matrix $\mathbf{C}_2$ in (17), we obtain from (18) that

$$\mathbf{Q}_y = \mathbf{C}_2\mathbf{Q}_x\mathbf{C}_2^\top = \begin{bmatrix} \widetilde{\mathbf{C}}^\top\mathbf{M}^{-1/2}\hat{\mathbf{U}}\mathbf{G}\hat{\mathbf{U}}^\top\mathbf{M}^{-1/2}\widetilde{\mathbf{C}} & \widetilde{\mathbf{C}}^\top\mathbf{M}^{-1/2}\hat{\mathbf{U}}\mathbf{S}\mathbf{U}^\top\mathbf{M}^{-1/2} \\ \mathbf{M}^{-1/2}\mathbf{U}\mathbf{S}^\top\hat{\mathbf{U}}^\top\mathbf{M}^{-1/2}\widetilde{\mathbf{C}} & \mathbf{M}^{-1/2}\mathbf{U}\mathbf{R}\mathbf{U}^\top\mathbf{M}^{-1/2} \end{bmatrix}.$$

With the block matrices $\mathbf{A}_2$ and $\mathbf{B}_2$ in (52) and the blocks $\mathbf{A}_{22}$, $\mathbf{A}_{23}$, $\mathbf{A}_{24}$ and $\mathbf{B}_{22}$ in (53) and the block matrix $\mathbf{Q}_x$ in (26), we derive from the Lyapunov Eq. (19) that

$$\begin{bmatrix} \mathbf{0} & \mathbf{A}_{22} \\ \mathbf{A}_{23} & \mathbf{A}_{24} \end{bmatrix}\begin{bmatrix} \mathbf{G} & \mathbf{S} \\ \mathbf{S}^\top & \mathbf{R} \end{bmatrix} + \begin{bmatrix} \mathbf{G} & \mathbf{S} \\ \mathbf{S}^\top & \mathbf{R} \end{bmatrix}\begin{bmatrix} \mathbf{0} & \mathbf{A}_{22} \\ \mathbf{A}_{23} & \mathbf{A}_{24} \end{bmatrix}^\top + \begin{bmatrix} \mathbf{0} \\ \mathbf{B}_{22} \end{bmatrix}\begin{bmatrix} \mathbf{0} & \mathbf{B}_{22}^\top \end{bmatrix} = \mathbf{0},$$

which yields

$$\mathbf{S}\mathbf{A}_{22}^\top + \mathbf{A}_{22}\mathbf{S}^\top = \mathbf{0}, \tag{54a}$$

$$\mathbf{G}\mathbf{A}_{23}^\top + \mathbf{S}\mathbf{A}_{24}^\top + \mathbf{A}_{22}\mathbf{R} = \mathbf{0}, \tag{54b}$$

$$\mathbf{S}^\top\mathbf{A}_{23}^\top + \mathbf{R}\mathbf{A}_{24}^\top + \mathbf{A}_{23}\mathbf{S} + \mathbf{A}_{24}\mathbf{R} = -\mathbf{B}_{22}\mathbf{B}_{22}^\top. \tag{54c}$$

Denote $\mathbf{S} = \begin{bmatrix}\mathbf{S}_1 & \mathbf{S}_2\end{bmatrix}$ with $\mathbf{S}_1 \in \mathbb{R}^{n-1}$ and $\mathbf{S}_2 \in \mathbb{R}^{(n-1)\times(n-1)}$ and insert it into (54a), then

$$\begin{bmatrix}\mathbf{S}_1 & \mathbf{S}_2\end{bmatrix}\begin{bmatrix}\mathbf{0}\\ \mathbf{I}_{n-1}\end{bmatrix} + \begin{bmatrix}\mathbf{0} & \mathbf{I}_{n-1}\end{bmatrix}\begin{bmatrix}\mathbf{S}_1^\top\\ \mathbf{S}_2^\top\end{bmatrix} = \mathbf{0}, \tag{55}$$

which leads to

$$\mathbf{S}_2 + \mathbf{S}_2^\top = \mathbf{0},$$

which means that $\mathbf{S}_2$ is a skew-symmetric matrix. Thus, the elements of $\mathbf{S}$ satisfy

$$s_{j-1,i+1} = -s_{i,j}, i = 1, 2, \dots, n-1,\ \ j = 2, \dots, n.$$

It yields from Assumption 4.1 and (53) that $\mathbf{A}_{24} = -\alpha\mathbf{I}_n$. Hence, we obtain from (54b) and (54c) that

$$\alpha\mathbf{S} = \mathbf{G}\mathbf{A}_{23}^\top + \mathbf{A}_{22}\mathbf{R}, \tag{56a}$$

$$2\alpha\mathbf{R} = \mathbf{S}^\top\mathbf{A}_{23}^\top + \mathbf{A}_{23}\mathbf{S} + \mathbf{B}_{22}\mathbf{B}_{22}^\top. \tag{56b}$$

By inserting (56b) into (56a), we derive

$$\begin{aligned}2\alpha^2\mathbf{S} &= 2\alpha\mathbf{G}\mathbf{A}_{23}^\top + \mathbf{A}_{22}\mathbf{S}^\top\mathbf{A}_{23}^\top + \mathbf{A}_{22}\mathbf{A}_{23}\mathbf{S} + \mathbf{A}_{22}\mathbf{B}_{22}\mathbf{B}_{22}^\top\\ &\quad \text{by (54a)}\\ &= 2\alpha\mathbf{G}\mathbf{A}_{23}^\top - \mathbf{S}\mathbf{A}_{22}^\top\mathbf{A}_{23}^\top + \mathbf{A}_{22}\mathbf{A}_{23}\mathbf{S} + \mathbf{A}_{22}\mathbf{B}_{22}\mathbf{B}_{22}^\top.\end{aligned}$$

Plugging $\mathbf{A}_{23}$ and $\mathbf{A}_{22}$ of (53) into the above equation, we get

$$2\alpha\mathbf{G}\begin{bmatrix}\mathbf{0} & -\boldsymbol{\Lambda}_{n-1}\end{bmatrix} + \begin{bmatrix}\mathbf{0} & \mathbf{I}_{n-1}\end{bmatrix}\mathbf{B}_{22}\mathbf{B}_{22}^\top = 2\alpha^2\mathbf{S} + \mathbf{S}\begin{bmatrix}\mathbf{0} & \mathbf{0}\\ \mathbf{0} & -\boldsymbol{\Lambda}_{n-1}\end{bmatrix} + \boldsymbol{\Lambda}_{n-1}\mathbf{S}.$$

With the notation of $\mathbf{S} = \begin{bmatrix}\mathbf{S}_1 & \mathbf{S}_2\end{bmatrix}$, we obtain from the above equation that

$$\begin{aligned}&\begin{bmatrix}\mathbf{0} & -2\alpha\mathbf{G}\boldsymbol{\Lambda}_{n-1}\end{bmatrix} + \begin{bmatrix}\mathbf{0} & \mathbf{I}_{n-1}\end{bmatrix}\mathbf{B}_{22}\mathbf{B}_{22}^\top\\ &= 2\alpha^2\begin{bmatrix}\mathbf{S}_1 & \mathbf{S}_2\end{bmatrix} + \begin{bmatrix}\boldsymbol{\Lambda}_{n-1}\mathbf{S}_1 & \boldsymbol{\Lambda}_{n-1}\mathbf{S}_2\end{bmatrix} + \begin{bmatrix}\mathbf{0} & -\mathbf{S}_2\boldsymbol{\Lambda}_{n-1}\end{bmatrix}\\ &= \begin{bmatrix}2\alpha^2\mathbf{S}_1 + \boldsymbol{\Lambda}_{n-1}\mathbf{S}_1 & 2\alpha^2\mathbf{S}_2 + \boldsymbol{\Lambda}_{n-1}\mathbf{S}_2 - \mathbf{S}_2\boldsymbol{\Lambda}_{n-1}\end{bmatrix}.\end{aligned} \tag{57}$$

From the definition of $\mathbf{B}_{22}$ in (53), we obtain

$$\begin{bmatrix}\mathbf{0} & \mathbf{I}_{n-1}\end{bmatrix}\mathbf{B}_{22}\mathbf{B}_{22}^\top = \begin{bmatrix}\sum_k u_{k,2}u_{k,1}\xi_k & \sum_k u_{k,2}^2\xi_k & \cdots & \sum_k u_{k,2}u_{k,n}\xi_k\\ \sum_k u_{k,3}u_{k,1}\xi_k & \sum_k u_{k,3}u_{k,2}\xi_k & \cdots & \sum_k u_{k,3}u_{k,n}\xi_k\\ \vdots & \vdots & \vdots & \vdots\\ \sum_k u_{k,n}u_{k,1}\xi_k & \sum_k u_{k,n}u_{k,2}\xi_k & \cdots & \sum_k u_{k,n}^2\xi_k\end{bmatrix}, \tag{58}$$

where $u_{i,j}$ is the element of the matrix $\mathbf{U}$ and ξ_k represent the kth diagonal elements in $\mathbf{M}^{-1/2}\widetilde{\mathbf{B}}^2\mathbf{M}^{-1/2}$. Plugging (58) into (57), we obtain that the elements of the vector $2\alpha^2\mathbf{S}_1 + \boldsymbol{\Lambda}_{n-1}\mathbf{S}_1$ satisfy

$$\begin{bmatrix}(2\alpha^2+\lambda_2)s_{1,1}\\ (2\alpha^2+\lambda_3)s_{2,1}\\ \vdots\\ (2\alpha^2+\lambda_n)s_{n-1,1}\end{bmatrix} = \begin{bmatrix}\sum_k u_{k,2}u_{k,1}\xi_k\\ \sum_k u_{k,3}u_{k,1}\xi_k\\ \vdots\\ \sum_k u_{k,n}u_{k,1}\xi_k\end{bmatrix},$$

which yields (28). Similarly, the elements of the matrix $2\alpha^2\mathbf{S}_2 + \boldsymbol{\Lambda}_{n-1}\mathbf{S}_2 - \mathbf{S}_2\boldsymbol{\Lambda}_{n-1}$ satisfy

$$\begin{aligned}&\begin{bmatrix}0 & (-2\alpha^2-\lambda_2+\lambda_3)s_{2,2} & \cdots & (-2\alpha^2-\lambda_2+\lambda_n)s_{n-1,2}\\ (2\alpha^2+\lambda_3-\lambda_2)s_{2,2} & 0 & \cdots & (-2\alpha^2-\lambda_3+\lambda_n)s_{n-1,3}\\ \vdots & \vdots & \vdots & \vdots\\ (2\alpha^2+\lambda_n-\lambda_2)s_{n-1,2} & (2\alpha^2+\lambda_n-\lambda_3)s_{n-1,3} & \cdots & 0\end{bmatrix}\\ &= \begin{bmatrix}\sum_k u_{k,2}^2\xi_k & \sum_k u_{k,2}u_{k,3}\xi_k & \cdots & \sum_k u_{k,2}u_{k,n}\xi_k\\ \sum_k u_{k,3}u_{k,2}\xi_k & \sum_k u_{k,3}^2\xi_k & \cdots & \sum_k u_{k,3}u_{k,n}\xi_k\\ \vdots & \vdots & \vdots & \vdots\\ \sum_k u_{k,n}u_{k,2}\xi_k & \sum_k u_{k,n}u_{k,3}\xi_k & \cdots & \sum_k u_{k,n}^2\xi_k\end{bmatrix}\\ &\quad - 2\alpha\begin{bmatrix}\lambda_2 g_{1,1} & \lambda_3 g_{1,2} & \cdots & \lambda_n g_{1,n-1}\\ \lambda_2 g_{2,1} & \lambda_3 g_{2,2} & \cdots & \lambda_n g_{2,n-1}\\ \vdots & \vdots & \vdots & \vdots\\ \lambda_2 g_{n-1,1} & \lambda_3 g_{n-1,2} & \cdots & \lambda_n g_{n-1,n-1}\end{bmatrix}.\end{aligned} \tag{59}$$

By the symmetry of $\mathbf{G}$, i.e., $g_{i,j} = g_{j,i}$, we obtain from (59) that for $i = 1, 2, \dots, n-1, j = 2, \dots, n$,

$$\left(2 - \frac{2\alpha^2}{\lambda_{i+1}} - \frac{2\alpha^2}{\lambda_j} - \frac{\lambda_{i+1}}{\lambda_j} - \frac{\lambda_j}{\lambda_{i+1}}\right)s_{i,j} = \left(\frac{1}{\lambda_{i+1}} - \frac{1}{\lambda_j}\right)\mathbf{u}_{i+1}^\top\mathbf{M}^{-1/2}\widetilde{\mathbf{B}}^2\mathbf{M}^{-1/2}\mathbf{u}_j, \tag{60}$$

which yields (29).

From (59), we obtain for $i = 1, 2, \dots, n-1$,

$$g_{i,i} = \frac{1}{2\alpha\lambda_{i+1}}\mathbf{u}_{i+1}^\top\mathbf{M}^{-1/2}\widetilde{\mathbf{B}}^2\mathbf{M}^{-1/2}\mathbf{u}_{i+1}, \tag{61}$$

and for $i = 1, 2, \dots, n-1, j = i+1, \dots, n-1$,

$$-2\alpha\lambda_{j+1}g_{i,j} = (\lambda_{j+1} - \lambda_{i+1} - 2\alpha^2)s_{j,i+1} - \mathbf{u}_{i+1}^\top\mathbf{M}^{-1/2}\widetilde{\mathbf{B}}^2\mathbf{M}^{-1/2}\mathbf{u}_{j+1}, \tag{62}$$

which yield (30) with the expression of $\mathbf{S}$ in (29).

Now, we focus on the derivation of $\mathbf{R}$. We denote

$$\mathbf{R} = \begin{bmatrix}R_1 & \mathbf{R}_2^\top\\ \mathbf{R}_2 & \mathbf{R}_3\end{bmatrix},$$

where $R_1 \in \mathbb{R}$, $\mathbf{R}_2 \in \mathbb{R}^{(n-1)}$ and $\mathbf{R}_3 \in \mathbb{R}^{(n-1)\times(n-1)}$. Then, (56b) is rewritten into

$$\begin{bmatrix}R_1 & \mathbf{R}_2^\top\\ \mathbf{R}_2 & \mathbf{R}_3\end{bmatrix} = \frac{1}{2\alpha}\left(\begin{bmatrix}0 & -\mathbf{S}_1^\top\boldsymbol{\Lambda}_{n-1}\\ -\boldsymbol{\Lambda}_{n-1}\mathbf{S}_1 & -\boldsymbol{\Lambda}_{n-1}\mathbf{S}_2 - \mathbf{S}_2^\top\boldsymbol{\Lambda}_{n-1}\end{bmatrix} + \mathbf{B}_{22}\mathbf{B}_{22}^\top\right), \tag{63}$$

where

$$\mathbf{B}_{22}\mathbf{B}_{22}^\top = \begin{bmatrix}\sum_k u_{k,1}^2\xi_k & \sum_k u_{k,1}u_{k,2}\xi_k & \cdots & \sum_k u_{k,1}u_{k,n}\xi_k\\ \sum_k u_{k,2}u_{k,1}\xi_k & \sum_k u_{k,2}^2\xi_k & \cdots & \sum_k u_{k,2}u_{k,n}\xi_k\\ \vdots & \vdots & \vdots & \vdots\\ \sum_k u_{k,n}u_{k,1}\xi_k & \sum_k u_{k,n}u_{k,2}\xi_k & \cdots & \sum_k u_{k,n}^2\xi_k\end{bmatrix}.$$

From (63), we obtain the expression of R_1 which equals to $r_{1,1}$ in (31). From (63), we obtain,

$$\mathbf{R}_2 = \frac{1}{2\alpha}\left(-\begin{bmatrix}\lambda_2 s_{1,1}\\ \lambda_3 s_{2,1}\\ \vdots\\ \lambda_n s_{n-1,1}\end{bmatrix} + \begin{bmatrix}\sum_k u_{k,1}u_{k,2}\xi_k\\ \sum_k u_{k,1}u_{k,3}\xi_k\\ \vdots\\ \sum_k u_{k,1}u_{k,n}\xi_k\end{bmatrix}\right),$$

from which we obtain for $i = 1, 2, \dots, n-1$,

$$r_{i+1,1} = \frac{1}{2\alpha}(-\lambda_{i+1}s_{i,1} + \mathbf{u}_{i+1}^\top\boldsymbol{M}^{-1/2}\widetilde{\mathbf{B}}^2\mathbf{M}^{-1/2}\mathbf{u}_1), \tag{64}$$

which leads (32) with the expression of $s_{i,1}$ in (28).

From (63), we further obtain,

$$2\alpha\mathbf{R}_3=\begin{bmatrix}\sum_k u_{k,2}^2\xi_k & \sum_k u_{k,2}u_{k,3}\xi_k & \cdots & \sum_k u_{k,2}u_{k,n}\xi_k\\ \sum_k u_{k,3}u_{k,2}\xi_k & \sum_k u_{k,3}^2\xi_k & \cdots & \sum_k u_{k,3}u_{k,n}\xi_k\\ \vdots & \vdots & \vdots & \vdots\\ \sum_k u_{k,n}u_{k,2}\xi_k & \sum_k u_{k,n}u_{k,3}\xi_k & \cdots & \sum_k u_{k,n}^2\xi_k\end{bmatrix}+\begin{bmatrix}0 & (\lambda_2-\lambda_3)s_{2,2} & \cdots & (\lambda_2-\lambda_n)s_{n-1,2}\\ (-\lambda_3+\lambda_2)s_{2,2} & 0 & \cdots & (\lambda_3-\lambda_n)s_{n-1,3}\\ \vdots & \vdots & \vdots & \vdots\\ (-\lambda_n+\lambda_2)s_{n-1,2} & (-\lambda_n+\lambda_3)s_{n-1,3} & \cdots & 0\end{bmatrix}. \tag{65}$$

Thus, for $i,j=2,3,\dots,n$,

$$r_{i,j}=\frac{1}{2\alpha}\left((\lambda_i-\lambda_j)s_{j-1,i}+\mathbf{u}_i^{\mathsf{T}}\mathbf{M}^{-1/2}\widetilde{\mathbf{B}}^2\mathbf{M}^{-1/2}\mathbf{u}_j\right),$$

which leads to (32) with the formula of $s_{j-1,i}$ in (29). □

Proof of Proposition 4.6. Following (A.1) in the Appendix and Assumptions 4.3 and 4.5, we obtain the eigenvalues of the matrix $\mathbf{M}^{-1/2}\mathbf{L}\mathbf{M}^{-1/2}$ as defined in (14), which satisfy

$$\lambda_1=0,\lambda_i=\gamma\eta^{-1}n,\ \text{for } i=2,\dots,n.$$

With these eigenvalues and Theorem 4.2, the formula of $\mathbf{R}$ is rewritten into

$$\mathbf{R}=\eta^{-1}\begin{bmatrix}\frac{1}{2\alpha}\mathbf{u}_1^{\mathsf{T}}\widetilde{\mathbf{B}}^2\mathbf{u}_1 & \frac{\alpha}{2\alpha^2+\eta^{-1}\gamma n}\mathbf{u}_1^{\mathsf{T}}\widetilde{\mathbf{B}}^2\widehat{\mathbf{U}}\\ \frac{\alpha}{2\alpha^2+\eta^{-1}\gamma n}\widehat{\mathbf{U}}^{\mathsf{T}}\widetilde{\mathbf{B}}\mathbf{u}_1 & \frac{1}{2\alpha}\widehat{\mathbf{U}}^{\mathsf{T}}\widetilde{\mathbf{B}}^2\widehat{\mathbf{U}}\end{bmatrix}. \tag{66}$$

Hence, the variance matrix of frequency satisfies

$$\begin{aligned}\mathbf{Q}_\omega&=\eta^{-1}\begin{bmatrix}\mathbf{u}_1 & \widehat{\mathbf{U}}\end{bmatrix}\mathbf{R}\begin{bmatrix}\mathbf{u}_1 & \widehat{\mathbf{U}}\end{bmatrix}^{\mathsf{T}}\\ &\text{by }\ \mathbf{u}_1\mathbf{u}_1^{\mathsf{T}}+\widehat{\mathbf{U}}\widehat{\mathbf{U}}^{\mathsf{T}}=\mathbf{I}\\ &=\eta^{-2}\left(\frac{1}{2\alpha}\widetilde{\mathbf{B}}^2+\left(\frac{\alpha}{2\alpha^2+\eta^{-1}\gamma n}-\frac{1}{2\alpha}\right)\left(\mathbf{u}_1\mathbf{u}_1^{\mathsf{T}}\widetilde{\mathbf{B}}^2+\widetilde{\mathbf{B}}^2\mathbf{u}_1\mathbf{u}_1^{\mathsf{T}}\right)\right.\\ &\quad\left.+\left(\frac{1}{\alpha}-\frac{2\alpha}{2\alpha^2+\eta^{-1}\gamma n}\right)\mathbf{u}_1\mathbf{u}_1^{\mathsf{T}}\widetilde{\mathbf{B}}^2\mathbf{u}_1\mathbf{u}_1^{\mathsf{T}}\right).\end{aligned}$$

Inserting $\mathbf{u}_1=1/\sqrt{n}\mathbf{1}_n^{\mathsf{T}}$ into the above equation, we obtain the diagonal elements of $\mathbf{Q}_\omega$, which satisfy for $i=1,\dots,n$,

$$\begin{aligned}q_{\omega_{i,i}}&=\eta^{-2}\left(\frac{b_i^2}{2\alpha}+\frac{-\gamma b_i^2}{d(2\alpha^2+\eta^{-1}\gamma n)}+\frac{\gamma\,\mathrm{tr}\left(\widetilde{\mathbf{B}}^2\right)}{dn(2\alpha^2+\eta^{-1}\gamma n)}\right)\\ &=\left[\frac{1}{2d\eta}-\frac{\gamma(n-1)}{dn(2d^2+\gamma\eta n)}\right]b_i^2+\frac{\gamma(\mathrm{tr}(\widetilde{\mathbf{B}}^2)-b_i^2)}{dn\left(2d^2+\gamma\eta n\right)}.\end{aligned}$$

With the eigenvalues in (66) and the formula of $\mathbf{G}$ in (30), we derive

$$\mathbf{G}=\frac{1}{2\alpha\gamma n}\widehat{\mathbf{U}}^{\mathsf{T}}\widetilde{\mathbf{B}}^2\widehat{\mathbf{U}},$$

which is inserted into (27), we obtain

$$\begin{aligned}\mathbf{Q}_\delta=&\frac{1}{2\alpha\eta\gamma n}\widetilde{\mathbf{C}}^{\mathsf{T}}\widehat{\mathbf{U}}\widehat{\mathbf{U}}^{\mathsf{T}}\widetilde{\mathbf{B}}^2\widehat{\mathbf{U}}\widehat{\mathbf{U}}^{\mathsf{T}}\widetilde{\mathbf{C}}\\ &\text{by}[\mathbf{u}_1\ \ \widehat{\mathbf{U}}][\mathbf{u}_1\ \ \widehat{\mathbf{U}}]^{\mathsf{T}}=\mathbf{u}_1\mathbf{u}_1^{\mathsf{T}}+\widehat{\mathbf{U}}\widehat{\mathbf{U}}^{\mathsf{T}}=\mathbf{I}_n\\ =&\frac{1}{2d\gamma n}\widetilde{\mathbf{C}}^{\mathsf{T}}(\mathbf{I}_n-\mathbf{u}_1\mathbf{u}_1^{\mathsf{T}})\widetilde{\mathbf{B}}^2(\mathbf{I}_n-\mathbf{u}_1\mathbf{u}_1^{\mathsf{T}})\widetilde{\mathbf{C}}\\ &\text{by}\ \ \widetilde{\mathbf{C}}^{\mathsf{T}}\mathbf{u}_1=\mathbf{0}\\ =&\frac{1}{2d\gamma n}\widetilde{\mathbf{C}}^{\mathsf{T}}\widetilde{\mathbf{B}}^2\widetilde{\mathbf{C}},\end{aligned}$$

which leads to (34). If we substitute the formula of incidence matrix into the above equation, we will get (35). □

Proof of Proposition 4.8. Following Eq. (A.1) in the Appendix and the assumption of $\mathbf{D}=d\mathbf{I}$ and the weight $K_{i,j}\cos\delta_{ij}^*=\gamma$ for all the lines, we obtain the eigenvalues of the matrix $\mathbf{D}^{-1/2}\mathbf{L}\mathbf{D}^{-1/2}$,

$$\overline{\lambda}_1=0,\ \ \overline{\lambda}_i=n\gamma/d\ \text{ for } i=2,\dots,n.$$

Plugging these eigenvalues of the Laplacian matrix of the complete graph into (24), we obtain the expression of the elements of the matrix $\overline{\mathbf{Q}}_x$,

$$\overline{q}_{x_{ij}}=\frac{1}{2\gamma n}\overline{\mathbf{u}}_{i+1}^{\mathsf{T}}\widetilde{\mathbf{B}}^2\overline{\mathbf{u}}_{j+1},\ \forall i,\ j=1,\dots,n-1.$$

Thus, $\overline{\mathbf{Q}}_x=\frac{1}{2\gamma n}\overline{\mathbf{U}}_2^{\mathsf{T}}\widetilde{\mathbf{B}}^2\overline{\mathbf{U}}_2$. Following (22), we derive

$$\begin{aligned}\overline{\mathbf{Q}}_y&=\frac{1}{2d\gamma n}\widetilde{\mathbf{C}}^{\mathsf{T}}\overline{\mathbf{U}}_2\overline{\mathbf{U}}_2^{\mathsf{T}}\widetilde{\mathbf{B}}^2\overline{\mathbf{U}}_2\overline{\mathbf{U}}_2^{\mathsf{T}}\widetilde{\mathbf{C}}=\frac{1}{2d\gamma n}\widetilde{\mathbf{C}}^{\mathsf{T}}(\mathbf{I}-\overline{\mathbf{u}}_1\overline{\mathbf{u}}_1^{\mathsf{T}})\widetilde{\mathbf{B}}^2(\mathbf{I}-\overline{\mathbf{u}}_1\overline{\mathbf{u}}_1^{\mathsf{T}})\widetilde{\mathbf{C}}\\ &=\frac{1}{2d\gamma n}\widetilde{\mathbf{C}}^{\mathsf{T}}\widetilde{\mathbf{B}}^2\widetilde{\mathbf{C}},\end{aligned}$$

which completes the proof. □

Proof of Proposition 4.9. The proof is in analogy to the one for Proposition 4.6 with the explicit formulas of the eigenvalues of the Laplacian matrix of a star graph in (A.2). For details of the proof, we refer to the arXiv version of this paper [41].

Proof of Proposition 4.12.

Following Eq. (A.2) in the Appendix and the assumption of $\mathbf{D}=d\mathbf{I}$ and $l_{c_{i,j}}=\gamma$ for all the lines, we obtain the eigenvalues of the matrix $\mathbf{D}^{-1/2}\mathbf{L}\mathbf{D}^{-1/2}$,

$$\overline{\lambda}_1=0,\ \ \overline{\lambda}_2=\cdots=\overline{\lambda}_{n-1}=\gamma/d,\ \ \overline{\lambda}_n=n\gamma/d\ \text{ for } i=2,\dots,n.$$

Following the formula of the matrix $\overline{\mathbf{Q}}_x$ in (24), we obtain,

$$\overline{q}_{x_{i,j}}=\begin{cases}\frac{1}{2\gamma}\overline{\mathbf{u}}_i^{\mathsf{T}}\widetilde{\mathbf{B}}^2\overline{\mathbf{u}}_j, & i,j=2,\dots,n-1,\\ \frac{1}{\gamma(1+n)}\overline{\mathbf{u}}_n^{\mathsf{T}}\widetilde{\mathbf{B}}^2\overline{\mathbf{u}}_j, & i=n,j=2,\dots,n-1,\\ \frac{1}{\gamma(1+n)}\overline{\mathbf{u}}_i^{\mathsf{T}}\widetilde{\mathbf{B}}^2\overline{\mathbf{u}}_n, & j=n,i=2,\dots,n-1,\\ \frac{1}{2\gamma n}\overline{\mathbf{u}}_n^{\mathsf{T}}\widetilde{\mathbf{B}}^2\overline{\mathbf{u}}_n, & i=j=n.\end{cases} \tag{67}$$

Denote $\overline{\mathbf{U}}_2=[\widehat{\overline{\mathbf{U}}}_2\ \ \overline{\mathbf{u}}_n]$, where $\widehat{\overline{\mathbf{U}}}_2\in\mathbb{R}^{n\times(n-2)}$. Then we convert the matrix $\overline{\mathbf{Q}}_x$ into four blocks,

$$\overline{\mathbf{Q}}_x=\begin{bmatrix}\frac{1}{2\gamma}\widehat{\overline{\mathbf{U}}}_2^{\mathsf{T}}\widetilde{\mathbf{B}}^2\widehat{\overline{\mathbf{U}}}_2 & \frac{1}{\gamma(1+n)}\widehat{\overline{\mathbf{U}}}_2^{\mathsf{T}}\widetilde{\mathbf{B}}^2\overline{\mathbf{u}}_n\\ \frac{1}{\gamma(1+n)}\overline{\mathbf{u}}_n^{\mathsf{T}}\widetilde{\mathbf{B}}^2\widehat{\overline{\mathbf{U}}}_2 & \frac{1}{2\gamma n}\overline{\mathbf{u}}_n^{\mathsf{T}}\widetilde{\mathbf{B}}^2\overline{\mathbf{u}}_n\end{bmatrix}.$$

Let $\widetilde{\mathbf{T}}=\overline{\mathbf{U}}_2\overline{\mathbf{Q}}_x\overline{\mathbf{U}}_2^{\mathsf{T}}$, then we have

$$\begin{aligned}\widetilde{\mathbf{T}}=&[\widehat{\overline{\mathbf{U}}}_2\ \ \overline{\mathbf{u}}_n]\begin{bmatrix}\frac{1}{2\gamma}\widehat{\overline{\mathbf{U}}}_2^{\mathsf{T}}\widetilde{\mathbf{B}}^2\widehat{\overline{\mathbf{U}}}_2 & \frac{1}{\gamma(1+n)}\widehat{\overline{\mathbf{U}}}_2^{\mathsf{T}}\widetilde{\mathbf{B}}^2\overline{\mathbf{u}}_n\widetilde{\mathbf{C}}\\ \frac{1}{\gamma(1+n)}\overline{\mathbf{u}}_n^{\mathsf{T}}\widetilde{\mathbf{B}}^2\widehat{\overline{\mathbf{U}}}_2 & \frac{1}{2\gamma n}\overline{\mathbf{u}}_n^{\mathsf{T}}\widetilde{\mathbf{B}}^2\overline{\mathbf{u}}_n\end{bmatrix}[\widehat{\overline{\mathbf{U}}}_2\ \ \overline{\mathbf{u}}_n]^{\mathsf{T}}\\ =&\frac{1}{2\gamma}\widetilde{\mathbf{B}}^2+\frac{1}{2\gamma}\left(\overline{\mathbf{u}}_1\overline{\mathbf{u}}_1^{\mathsf{T}}\widetilde{\mathbf{B}}^2\overline{\mathbf{u}}_1\overline{\mathbf{u}}_1^{\mathsf{T}}-\overline{\mathbf{u}}_1\overline{\mathbf{u}}_1^{\mathsf{T}}\widetilde{\mathbf{B}}^2-\widetilde{\mathbf{B}}^2\overline{\mathbf{u}}_1\overline{\mathbf{u}}_1^{\mathsf{T}}\right)+\frac{(n-1)^2}{2\gamma n(1+n)}\overline{\mathbf{u}}_n\overline{\mathbf{u}}_n^{\mathsf{T}}\widetilde{\mathbf{B}}^2\overline{\mathbf{u}}_n\overline{\mathbf{u}}_n^{\mathsf{T}}\\ &+\frac{n-1}{2\gamma(1+n)}\left(\overline{\mathbf{u}}_1\overline{\mathbf{u}}_1^{\mathsf{T}}\widetilde{\mathbf{B}}^2\overline{\mathbf{u}}_n\overline{\mathbf{u}}_n^{\mathsf{T}}+\overline{\mathbf{u}}_n\overline{\mathbf{u}}_n^{\mathsf{T}}\widetilde{\mathbf{B}}^2\overline{\mathbf{u}}_1\overline{\mathbf{u}}_1^{\mathsf{T}}-\widetilde{\mathbf{B}}^2\overline{\mathbf{u}}_n\overline{\mathbf{u}}_n^{\mathsf{T}}-\overline{\mathbf{u}}_n\overline{\mathbf{u}}_n^{\mathsf{T}}\widetilde{\mathbf{B}}^2\right).\end{aligned}$$

So we get the formula of the variance matrix of the phase differences,

$$\overline{\mathbf{Q}}_\delta=\frac{1}{d}\widetilde{\mathbf{C}}^{\mathsf{T}}\widetilde{\mathbf{T}}\widetilde{\mathbf{C}},$$

and substitute the incidence matrix $\widetilde{\mathbf{C}}$ into the above equation, we have

$$\overline{q}_{\delta_{k,q}}=\frac{1}{d}\left(\widetilde{T}_{11}-\widetilde{T}_{k+1,1}-\widetilde{T}_{1,q+1}+\widetilde{T}_{k+1,q+1}\right).$$

Following Eq. (A.2) in the Appendix, the vector $\overline{\mathbf{u}}_n=1/\sqrt{n(n-1)}[1-n,1,\dots,1]^{\mathsf{T}}$ is the eigenvector corresponding to the eigenvalue n, then

we obtain,

$$\widetilde{T}_{11} = \frac{1}{2\gamma} b_1^2 + \frac{1}{2\gamma n^3(1+n)} \left[(1-n)^4 b_1^2 + (1-n)^2 \sum_{t=2}^{n} b_t^2 \right] + \frac{1}{2\gamma} \left(\frac{1}{n^2} \mathrm{tr}\left(\widetilde{\mathbf{B}}^2\right) - \frac{2}{n} b_1^2 \right) + \frac{1}{2\gamma n^2(1+n)} \left(2(1-n)^2 b_1^2 + 2(1-n) \sum_{t=2}^{n} b_t^2 - 2n(1-n)^2 b_1^2 \right),$$

$$\widetilde{T}_{1,q+1} = \frac{1}{2\gamma n^3(1+n)} \left[(1-n)^3 b_1^2 + (1-n) \sum_{t=2}^{n} b_t^2 \right] + \frac{1}{2\gamma} \left(\frac{1}{n^2} \mathrm{tr}\left(\widetilde{\mathbf{B}}^2\right) - \frac{b_1^2 + b_{q+1}^2}{n} \right) + \frac{1}{2\gamma n^2(1+n)} \left((2-n)(1-n) b_1^2 + (2-n) \sum_{t=2}^{n} b_t^2 - n(1-n) b_1^2 - n(1-n) b_{q+1}^2 \right),$$

$$\widetilde{T}_{k+1,1} = \frac{1}{2\gamma n^3(1+n)} \left[(1-n)^3 b_1^2 + (1-n) \sum_{t=2}^{n} b_t^2 \right] + \frac{1}{2\gamma} \left(\frac{1}{n^2} \mathrm{tr}\left(\widetilde{\mathbf{B}}^2\right) - \frac{b_1^2 + b_{k+1}^2}{n} \right) + \frac{1}{2\gamma n^2(1+n)} \left((2-n)(1-n) b_1^2 + (1-n) \sum_{t=2}^{n} b_t^2 + (2-n) b_1^2 - n(1-n) b_{k+1}^2 \right),$$

$$\widetilde{T}_{k+1,q+1} = \frac{1}{2\gamma n^3(1+n)} \left[(1-n)^2 b_1^2 + \sum_{t=2}^{n} b_t^2 \right] + \frac{1}{2\gamma} \left(\frac{1}{n^2} \mathrm{tr}\left(\widetilde{\mathbf{B}}^2\right) - \frac{b_{q+1}^2 + b_{k+1}^2}{n} \right) + \frac{1}{2\gamma n^2(1+n)} \left(2(1-n) b_1^2 + 2 \sum_{t=2}^{n} b_t^2 - n(b_{k+1}^2 + b_{q+1}^2) \right), \ (k \neq q),$$

$$\widetilde{T}_{k+1,k+1} = \frac{1}{2\gamma} b_{k+1}^2 + \frac{1}{2\gamma n^3(1+n)} \left[(1-n)^2 b_1^2 + \sum_{t=2}^{n} b_t^2 \right] + \frac{1}{2\gamma n^2(1+n)} \left(2(1-n) b_1^2 + 2 \sum_{t=2}^{n} b_t^2 - 2n b_{k+1}^2 \right) + \frac{1}{2\gamma} \left(\frac{1}{n^2} \mathrm{tr}\left(\widetilde{\mathbf{B}}^2\right) - \frac{2 b_{k+1}^2}{n} \right).$$

With these formulas, we further obtain

$$\overline{q}_{\delta_{k,q}} = \frac{1}{d} \left(\widetilde{T}_{11} - \widetilde{T}_{k+1,1} - \widetilde{T}_{1,q+1} + \widetilde{T}_{k+1,q+1} \right),$$

and

$$\overline{q}_{\delta_{k,k}} = \frac{1}{d} \left(\widetilde{T}_{11} - \widetilde{T}_{k+1,1} - \widetilde{T}_{1,k+1} + \widetilde{T}_{k+1,k+1} \right),$$

which leads to (50) and (51) respectively. □

6. Conclusions

The explicit formula of the variance matrix of a linearized stochastic system of a power system has been deduced at the invariant probability distribution based on the assumption of uniform damping-inertia ratio at all nodes. With this analytic formula and assumption of identical weights of the lines, the impact of the system parameters on the propagation of the fluctuations in the system with complete graphs and star graphs is analyzed. It is found that increasing the size of the network prevents the fluctuations from the source node of disturbances. This implies that adding a new node, which does help dissipate the fluctuations, prevents the fluctuations propagate from the disturbance's source node to other nodes. In addition, increasing the line capacity accelerates the fluctuation propagation in frequency and increasing the inertia also help suppress the fluctuation in the phase difference, both of which however is quite limited.

In the future, research interest remains on the analytic formula of the variance matrix without any assumptions on the system parameters. The results for different types of networks will be compared to reveal the impact of network topology on disturbance propagation. Attention will also be on the variance matrices of the systems with correlated disturbances.

CRediT authorship contribution statement

Xian Wu: Writing – original draft, Validation, Investigation, Formal analysis. **Kaihua Xi:** Writing – review & editing, Validation, Supervision, Investigation, Funding acquisition, Formal analysis, Conceptualization. **Aijie Cheng:** Supervision, Project administration. **Hai Xiang Lin:** Writing – review & editing, Supervision, Project administration. **Jan H. van Schuppen:** Writing – review & editing, Project administration, Conceptualization. **Chenghui Zhang:** Project administration, Funding acquisition.

Declaration of competing interest

The authors declare the following financial interests/personal relationships which may be considered as potential competing interests: Kaihua Xi reports financial support was provided by National Natural Science Foundation of China. Chenghui Zhang reports financial support was provided by National Natural Science Foundation of China. If there are other authors, they declare that they have no known competing financial interests or personal relationships that could have appeared to influence the work reported in this paper.

Data availability

Data will be made available on request.

Appendix

A.1. The spectrum of the Laplacian matrices

Consider the graph $\mathcal{G} = (\mathcal{V}, \mathcal{E})$. Assume the weights of all the lines are all identical, i.e., $w_{i,j} = \nu \in \mathbb{R}_+$ for $(i,j) \in \mathcal{E}$,

(i) If $\mathcal{G}$ is a complete graph, then the eigenvalues of the Laplacian matrix satisfy [42],

$$\mu_1 = 0, \text{ and } \mu_i = \nu n \text{ for } i = 2, \dots, n. \tag{A.1}$$

(ii) If $\mathcal{G}$ is a star graph, then the eigenvalues of the Laplacian matrix satisfy [42],

$$\mu_1 = 0, \mu_2 = \cdots = \mu_{n-1} = \nu, \mu_n = \nu n, \tag{A.2}$$

the vector $\begin{bmatrix} n-1 & -1 & -1 & \cdots & -1 \end{bmatrix}^\top \in \mathbb{R}^n$ is an eigenvector of the Laplacian matrix corresponding to the eigenvalue $\mu_n = \nu n$.

References

[1] Kundur P. Power system stability and control. New York: McGraw-Hill; 1994.
[2] Dörfler F, Bullo F. On the critical coupling for kuramoto oscillators. SIAM J Appl Dyn Syst 2011;10(3):1070–99.
[3] Jafarpour S, Huang EY, Smith KD, Bullo F. Flow and elastic networks on the n-torus: Geometry, analysis, and computation. SIAM Rev 2022;64(1):59–104.
[4] Skar S. Stability of multi-machine power systems with nontrivial transfer conductances. SIAM J Appl Math 1980;39(3):475–91.
[5] Motter AE, Myers SA, Anghel M, Nishikawa T. Spontaneous synchrony in power-grid networks. Nat Phys 2013;9(3):191–7.
[6] Menck PJ, Heitzig J, Kurths J, Joachim Schellnhuber H. How dead ends undermine power grid stability. Nature Commun 2014;5:3969.
[7] Delabays R, Tyloo M, Jacquod P. The size of the sync basin revisited. Chaos 2017;27(10):103109.
[8] Xi K, Dubbeldam JLA, Lin HX. Synchronization of cyclic power grids: Equilibria and stability of the synchronous state. Chaos 2017;27(1):013109.
[9] Poolla BK, Bolognani S, Dörfler F. Optimal placement of virtual inertia in power grids. IEEE Trans Autom Control 2017;62(12):6209–20.
[10] Xi K, Dubbeldam JL, Lin HX, van Schuppen JH. Power-imbalance allocation control of power systems-secondary frequency control. Automatica 2018;92:72–85.
[11] Fazlyab M, Dörfler F, Preciado VM. Optimal network design for synchronization of coupled oscillators. Automatica 2017;84:181–9.

[12] Tyloo M, Jacquod P. Primary control effort under fluctuating power generation in realistic high-voltage power networks. IEEE Control Syst Lett 2021;5(3):929–34.
[13] Tyloo M, Coletta T, Jacquod P. Robustness of synchrony in complex networks and generalized Kirchhoff indices. Phys Rev Lett 2018;120:084101.
[14] Tegling E, Bamieh B, Gayme DF. The price of synchrony: Evaluating the resistive losses in synchronizing power networks. IEEE Trans Control Netw Syst 2015;2(3):254–66.
[15] Coletta T, Jacquod P. Performance measures in electric power networks under line contingencies. IEEE Trans Control Netw Syst 2020;7(1):221–31.
[16] Grunberg TW, Gayme DF. Performance measures for linear oscillator networks over arbitrary graphs. IEEE Trans Control Netw Syst 2018;5(1):456–68.
[17] Paganini F, Mallada E. Global performance metrics for synchronization of heterogeneously rated power systems: The role of machine models and inertia. In: 2017 55th annual allerton conference on communication, control, and computing. 2017, p. 324–31.
[18] Jouini T, Sun Z. Performance analysis and optimization of power systems with spatially correlated noise. IEEE Control Syst Lett 2021;5(1):361–6.
[19] Coletta T, Bamieh B, Jacquod P. Transient performance of electric power networks under colored noise. In: 2018 IEEE conference on decision and control. 2018, p. 6163–7.
[20] Pagnier L, Jacquod P. Optimal placement of inertia and primary control: A matrix perturbation theory approach. IEEE Access 2019;7:145889–900.
[21] Pagnier P. Inertia location and slow network modes determine disturbance propagation in large-scale power grids. PLoS One 2019;14(3):1–17.
[22] Haehne H, Schmietendorf K, Tamrakar S, Peinke J, Kettemann S. Propagation of wind-power-induced fluctuations in power grids. Phys Rev E 2019;99:050301.
[23] Kettemann S. Delocalization of disturbances and the stability of AC electricity grids. Phys Rev E 2016;94:062311.
[24] Zhang X, Witthaut D, Timme M. Topological determinants of perturbation spreading in networks. Phys Rev Lett 2020;125:218301.
[25] Auer S, Hellmann F, Krause M, Kurths J. Stability of synchrony against local intermittent fluctuations in tree-like power grids. Chaos 2017;27(12):127003.
[26] Zhang X, Hallerberg S, Matthiae M, Witthaut D, Timme M. Fluctuation-induced distributed resonances in oscillatory networks. Sci Adv 2019;5(7):eaav1027.
[27] Manik D, Rohden M, Ronellenfitsch X, Hallerberg S, Witthaut D, et al. Network susceptibilities: Theory and applications. Phys Rev E 2017;95:012319.
[28] Wang Z, Xi K, Cheng A, Lin HX, Ran ACM, J HvS, et al. Synchronization of power systems under stochastic disturbances. Automatica 2023;151:110884.
[29] Adeen M, Bizzarri F, Giudice D, Grillo S, Linaro D, Brambilla A, Milano F. On the calculation of the variance of algebraic variables in power system dynamic models with stochastic processes. IEEE Trans Power Syst 2023;38(2):1739–42.
[30] Wu X, Xi K, Cheng A, Zhang C, Lin HX. A critical escape probability formulation for enhancing the transient stability of power systems with system parameter design. 2023, preprint, arXiv:2309.06803.
[31] Kwakernaak H, Sivan R. Linear optimal control systems. New York: Wiley-Interscience; 1972.
[32] Xi K, Wang Z, Cheng A, Lin HX, van Schuppen JH, Zhang C. Synchronization of complex network systems with stochastic disturbances. Siam J Appl Dyn Syst 2023;20(2):1030–52.
[33] Zaborszky J, Huang G, Zheng B, Leung TC. On the phase portrait of a class of large nonlinear dynamic systems such as the power system. IEEE Trans Autom Control 1988;33(1):4–15.
[34] Chiang HD, Hirsch M, Wu F. Stability regions of nonlinear autonomous dynamical systems. IEEE Trans Autom Control 1988;33(1):16–27.
[35] Dörfler F, Bullo F. Synchronization in complex networks of phase oscillators: A survey. Automatica 2014;50(6):1539–64.
[36] Bronski JC, DeVille L. Spectral theory for dynamics on graphs containing attractive and repulsive interactions. SIAM J Appl Math 2014;74(1):83–105.
[37] Zaborsky J, Huang G, Leung TC, Zheng B. Stability monitoring on the large electric power system. In: 24th IEEE conf. decision control, vol. 24. IEEE; 1985, p. 787–98.
[38] Karatzas I, Shreve S. Brownian motion and stochastic calculus. Berlin: Springer-Verlag; 1987.
[39] Dörfler F, Bullo F. Synchronization and transient stability in power networks and nonuniform kuramoto oscillators. SIAM J Control Optim 2012;50(3):1616–42.
[40] Kou G, Hadley SW, Markham PN, Liu Y. Developing Generic Dynamic Models for the 2030 Eastern Interconnection Grid.
[41] Wu X, Xi K, Cheng A, Lin HX, van Schuppen JH, Zhang C. Explicit formulas for the variance of the state of a linearized power system driven by Gaussian stochastic disturbances. 2023, preprint, arXiv:2302.06326.
[42] Mieghem PV. Graph spectra for complex networks. Vasa. Cambridge University Press; 2008.